

Multistage Interference Cancellation with Diversity Reception for Asynchronous QPSK DS/CDMA Systems over Multipath Fading Channels

Jianfeng Weng, Guoqiang Xue, Tho Le-Ngoc, and Sofiène Tahar

Dept. of Electrical & Computer Engineering, Concordia University, Canada

email: {jfweng, xue, tho, tahar}@ece.concordia.ca

Abstract

A multistage interference cancellation (MIC) technique with diversity reception for QPSK asynchronous Direct-Sequence Code-Division Multiple-Access (DS/CDMA) systems over frequency-selective multipath Rayleigh fading channels is introduced. Unlike the previous MIC [1, 2], which tries to remove the lump sum of the multiple-access interference (MAI) and self-interference (SI), this introduced MIC attempts to cancel only the MAI and part of the SI due to the inter-symbol interference, while treating the remaining SI created by the current symbol as a useful information for symbol decision. In this technique, the Rake combining is used to collect signal replicas over multiple fading paths. Upper and lower bounds on the bit error probability are derived using a Gaussian approximation and the characteristic function method. Furthermore, effects of channel estimation error on the performance are studied. Analytical and simulation results show that the introduced MIC can provide a performance extremely close to that in an ideal single-user environment, and outperforms the previous MIC even in the presence of channel estimation error.

1 Introduction

In personal and mobile communications, Direct-Sequence Code-Division Multiple-Access (DS/CDMA) technique [3, 4] has attracted a considerable attention due to its potential of high capacity and its robust performance in antijam and fading channels. In DS/CDMA system, multiple users are allowed to simultaneously occupy a common channel to transmit the information. To distinguish the transmitted information, users are assigned distinctive signature waveforms. The modulated signals from all users share the same channel and are present at the receiver. Due to a low mutual correlation between the signature waveforms, the target receiver can readily recover the information carried by the known signature waveform and treat the other users' signals as multiple access interference (MAI). In this way, communication between the transmitter and intended receiver can be

established despite the existing multiple users' signals in the common channel. However, the system performance may be degraded when the MAI becomes strong. Furthermore, interference from the high-power users can significantly corrupt the received signals of the low-power users and this is known as the "near/far" problem [3]. Accordingly, the system capacity would be limited. So far, to improve the multiple-access capability, much work has been done to alleviate the MAI, such as the power control and the use of quasi-orthogonal signature waveforms. Unfortunately, those remedies cannot totally eliminate the "near/far" shortcoming.

To circumvent the "near/far" problem, multiuser detection has been developed ever since Verdu [5] proposed the optimum multi-user detector to achieve the minimum bit error probability in asynchronous additive white Gaussian noise (AWGN). The optimum multiuser detection is basically a maximum likelihood sequence detector consisting of a bank of matched filters followed by a Viterbi algorithm. The required complexity is on the order of $O(2^K)$ for K active users and therefore it is undesirable for large K . To avoid the large computation, various efforts in designing sub-optimum multiuser detection have been conducted, such as the decorrelating detector [6], multi-stage detector [7], neural networks based detector [8], optimal bilinear detector [9], successive MAI cancellation [10], linear canceler [11], expectation-maximization (EM) based iterative receiver [12], and adaptive approaches [13, 14]. A comprehensive review of the recent multi-user detectors can be found in the literature [15]. Studies indicate that although these multiuser detectors vary in complexity, they can achieve a near single-user performance in AWGN channel by eliminating the MAI. On the other hand, when the system is operating in a multipath fading environment, the sum of the same information bearing signals through multiple fading paths but with different time delays and attenuation factors will be present at the receiver [3] and this incurs the self-interference (SI) apart from the MAI. To jointly suppress the MAI and the SI, the extension of the multiuser detection to the multipath fading channels has been studied [16–18]. In particular, Chen [16] studied a recursive least square (RLS) based decorrelating detector in synchronous BPSK system. Fawer and Aazhang [17] proposed a maximum-likelihood (ML) multiuser multipath detector for asynchronous BPSK and an EM based approach to solve the problem. In [18], Zvonar investigated a decorrelating approach in asynchronous BPSK and DPSK systems. Nevertheless, those detectors still require a large amount of computation especially when the numbers of active users and fading paths become large.

Among the multiuser detectors, multistage interference cancellation (MIC) [7, 10] has gained popularity due to its simplicity and flexibility. The MIC schemes considered in the literature can proceed serially (successively) [10] or in parallel [7]. In the serial MIC, the interference from other users is cancelled one by one from high-power to low-power users. Despite its simplicity, the serial MIC may incur the decision delay and it needs to know a specific geometric power distribution of all users [19]. Besides, the scheme is in favor of the low-power users and creates marginal benefits for the high-power users [20]. In the parallel MIC, however, all of the MAI for each user are simultaneously estimated and removed such that each user in the system is equally treated.

For this reason, in this paper, we focus on the parallel MIC. A further interesting feature of the MIC is that it provides tentative decisions in each stage so that it can meet variable requirements of users on the bit error rate (BER). For example, for users which could tolerate high bit error rate, we may stop in the initial stage to give an acceptable BER rather than perform additional stages of cancellation to achieve an unnecessarily low BER. Such feature is very interesting in the future joint voice/data applications [21, 22], where voice can tolerate higher bit error rates than data. Over the multipath fading channels, the extension of the parallel MIC to asynchronous BPSK over multipath fading channel can be found in [1, 2, 23]. Specifically, in [23], the MIC scheme was proposed to cancel the MAI alone, and a Rake receiver was simulated to estimate the channel parameters and to combine the fading replicas for symbol decision, while [1, 2] showed that the MIC could provide good performance by suppressing the lump sum of the MAI and the SI. It was also shown in [2] that by introducing a threshold to control the decision, a better performance could be achieved. However, no diversity technique was considered in [1, 2]. Furthermore, note that the SI is made up of the *self inter-symbol interference* (SII) incurred by the multipath components of the previous symbol and the *self current-symbol interference* (SCI) which corresponds to the current symbol. Due to the fact that the SCI contains the current symbol information which can be treated as a useful signal for symbol decision, the MIC can proceed with the *partial SI* cancellation to cancel the SII alone rather than the *full SI* cancellation.

In this work, we introduce the multistage interference cancellation with *partial SI* cancellation (MIC-PSI) and Rake combining and to study its performance in QPSK asynchronous DS/CDMA system over frequency-selective multipath Rayleigh fading channels. Here, QPSK modulation is considered instead of BPSK [1, 2, 23] due to its ability to achieve the same bit error probability using half the transmission bandwidth and its randomness property of rendering the signal more difficult to be detected by using feature detectors [3, 24]. Besides, QPSK spreading has been adopted in practical IS-95 CDMA digital cellular systems [24]. Through the work, we will focus on QPSK phase modulation and QPSK spreading. Furthermore, we still consider the hard symbol decision as in [1] due to the fact that the determination of an optimum threshold for the soft decision [2] is quite difficult in practice.

To evaluate the performance of the MIC-PSI, the upper and lower bounds on its probability of bit error in a multi-user environment are derived using a Gaussian approximation [1, 2] and the characteristic function method. The effects of channel estimation error on the performance are also studied. Analytical and simulation results show that the MIC-PSI can provide a performance extremely close to that in an ideal single-user system and outperforms the previous MIC with *full SI* cancellation (MIC-FSI) [1, 2]. Furthermore, even in the presence of channel estimation error, the MIC-PSI can offer a better performance.

The paper is organized as follows. In Section 2, the asynchronous QPSK DS/CDMA multiuser system in a frequency-selective multipath fading environment is described and modeled. Section 3 presents the multistage

interference cancellation scheme with the partial SI cancellation. In Section 4, the upper and lower bounds on the performance of the introduced MIC scheme are derived in both single-user and multiuser systems. Analytical and simulation results are illustrated and discussed in Section 5. Finally, Section 6 concludes the paper.

2 System Descriptions

We consider QPSK asynchronous DS/CDMA system with K active users over frequency-selective multipath Rayleigh fading channels. More precisely, we consider both QPSK modulation and QPSK spreading.

2.1 Transmitter model

There are a number of techniques to configure the *data* modulation and the *spreading*. For any user, if there is no restriction on the phase modulation, the balanced QPSK spreading model [24] can be used as illustrated in Fig. 1. The binary data bits are first passing through a phase modulator and the modulated signal is subsequently separated into two branches by a quadrature hybrid. Within the n -th symbol interval, the in-phase signal $\sqrt{\rho/N} \cos(\omega_0 t - \phi_n)$, and quadrature signal $\sqrt{\rho/N} \sin(\omega_0 t - \phi_n)$ are multiplied by the in-phase signature waveform $a^I(t)$ and quadrature-phase signature waveform $a^Q(t)$, respectively, where ω_0 is the carrier angular frequency and ϕ_n is the n -th information bearing phase shift taken from the set of $\{2\pi(m-1)/M, m = 1, 2, \dots, M\}$ for M-PSK modulation. Finally, the spread signals from two branches are summed to produce the transmitted signal,

$$S(t) = \sum_{n=-\infty}^{\infty} \left[\sqrt{\rho/N} a^I(t) \cos(\omega_0 t - \phi_n) - \sqrt{\rho/N} a^Q(t) \sin(\omega_0 t - \phi_n) \right] P_{T_b}(t - nT_b) \quad (1)$$

where ρ/N is the signal power and N is the length of the PN codes. $d^I(t) = \sum_{i=-\infty}^{\infty} a_i^I P_{T_c}(t - iT_c)$ and $a^Q(t) = \sum_{i=-\infty}^{\infty} a_i^Q P_{T_c}(t - iT_c)$. Here, a_i^I and a_i^Q are respectively the in-phase and quadrature-phase pseudo-random (PN) codes taken from the set $\{-1, 1\}$. For the code length N , $a_i^I = a_{N+i}^I$ and $a_i^Q = a_{N+i}^Q$. $P_T(t)$ denotes the unit rectangular pulse of duration T and $T_b = NT_c$.

By using the complex baseband signal representation [3], $S(t)$ in (1) can be expressed in the form of $S(t) = \text{Re} \{s(t)e^{j\omega_0 t}\}$, where $s(t)$ is the equivalent complex baseband signal from a user, i.e.,

$$s(t) = \sum_{n=-\infty}^{\infty} \sum_{i=-\infty}^{\infty} \sqrt{\rho/N} \left[a_i^I + ja_i^Q \right] e^{-j\phi_n} P_{T_b}(t - nT_b) P_{T_c}(t - iT_c) \quad (2)$$

When the in-phase and quadrature signature waveforms are identical, $s(t)$ in (2) simply reduces to the low-pass signal representation in [25]. Here, we consider a general case, in which the spreading uses different in-phase and quadrature signature waveforms.

In asynchronous system, the associated time delay and phase shift for each user should be included. For user k , the transmitted signal can be written as

$$s_k(t) = \sqrt{\frac{2\rho_k}{2N}} b_k(t - T^{(k)}) a_k(t - T^{(k)}) e^{j\theta_k} \quad (3)$$

where k is the user index, $\rho_k := E_k/N_o$ is the normalized signal power, in which E_k is the symbol energy and N_o is the noise power spectral density. $T^{(k)}$ is the associated time delay that can be either random or deterministic over $[0, T_b)$. θ_k is the phase shift and it is assumed to be uniformly distributed over $[0, 2\pi)$. The information bearing waveform $b_k(t)$ and the signature waveform $a_k(t)$ are

$$b_k(t) = \sum_{n=-\infty}^{\infty} e^{-j\phi_n^{(k)}} P_{T_b}(t - nT_b) \quad (4)$$

$$a_k(t) = \sum_{i=-\infty}^{\infty} [a_i^{(k),I} + ja_i^{(k),Q}] P_{T_c}(t - iT_c) \quad (5)$$

where $\phi_n^{(k)} \in \{2\pi(m-1)/4, m=1, 2, \dots, 4\}$ is the data bearing phase for QPSK phase modulation. $a_i^{(k),I} = a_{N+i}^{(k),I}$ and $a_i^{(k),Q} = a_{N+i}^{(k),Q}$ are respectively the in-phase and quadrature PN codes assigned to user k .

Accordingly, in an asynchronous multiuser system, the equivalent complex baseband signal model at the front-end of the receiver can be shown in Fig. 2, where the data signals of multiple users are modulated by the distinctive complex-valued signature waveforms $\{a_k(t - T^{(k)})\}$ and $h_k(t)$ denotes the impulse response of the channel for user k . In DS/CDMA system, the signal bandwidth is usually much larger than the coherence bandwidth of the channel and therefore the channel exhibits the frequency-selective characteristic [3].

2.2 Channel model

The equivalent lowpass impulse response of the channel for user k can be given by (see [1, 2, 17])

$$h_k(t) = \sum_{l=1}^{L_k} \alpha_l^{(k)} \delta(t - t_l^{(k)}) \quad (6)$$

where L_k is the number of paths which can be either random or deterministic. $\alpha_l^{(k)}$ and $t_l^{(k)}$ are respectively the fading parameter and the time delay in the l -th path of user k and they are assumed to be mutually statistically independent for all k and l . Let T_m be the maximum channel delay spread. Usually $T_m \ll T_b$ (the symbol duration) and $t_l^{(k)} < T_m$ for all l and k .

The fading parameter $\alpha_l^{(k)}$ in (6) is assumed to be zero-mean, complex-valued Gaussian random variable. In addition, the channel is considered to have a large coherence time, or equivalently a small Doppler spread [3], so that the fading parameter $\alpha_l^{(k)}$ exhibits a slowly changing characteristic and could be reliably estimated using a channel estimator.

2.3 Received signal model

As shown in Fig. 2, after passing through the channels, all the multiuser signals and the background noise will be present at the receiver. By using (3) and (6), the equivalent low-pass received signal, $r(t)$, can be written as

$$\begin{aligned} r(t) &= \sum_{k=1}^K \int_{-\infty}^{\infty} h_k(\tau) s_k(t - \tau) d\tau + z(t) \\ &= \sum_{k=1}^K \sqrt{\frac{2\rho_k}{2N}} \sum_{l=1}^{L_k} \alpha_l^{(k)} e^{j(\theta_k - \omega_0 \tau_l^{(k)})} b_k(t - \tau_l^{(k)}) a_k(t - \tau_l^{(k)}) + z(t) \end{aligned} \quad (7)$$

where $z(t)$ is the additive white Gaussian noise (AWGN) with zero mean and unit power spectral density. $\tau_l^{(k)} := T^{(k)} + t_l^{(k)}$, and $\omega_0 \tau_l^{(k)}$ is the phase shift incurred by the time delay $\tau_l^{(k)}$. $(\theta_k - \omega_0 \tau_l^{(k)})$ denotes the phase shift assumed to be uniformly distributed over $[0, 2\pi)$ [1]. Thus, in Rayleigh fading channels, $\alpha_l^{(k)} e^{j(\theta_k - \omega_0 \tau_l^{(k)})}$ in the above equation is still a zero-mean Gaussian random variable. Accordingly, in the following the carrier phase shift part $e^{j(\theta_k - \omega_0 \tau_l^{(k)})}$ can be absorbed into $\alpha_l^{(k)}$ without loss of generality.

The above models are similar to those in [1, 2], where the received signal from a single branch (the I branch) for BPSK case was considered. Here, we consider the received signals from both I and Q branches for QPSK modulation.

2.4 Channel estimation model

Before we proceed further, it is of interest to discuss the channel estimation model due to the fact that in reconstructing the interfering signals for the interference canceler, the knowledge of the fading parameters is required [1] while in practice, the channel knowledge is usually unknown *a priori* and should be estimated.

The channel estimation model can be established by considering separately the estimation errors in the signal amplitude and the carrier phase shift as in [1]. Here, for the sake of simplicity, we consider them jointly by assuming that the estimate of the complex-valued fading parameter is the actual value plus a complex-valued Gaussian disturbance. This consideration is also practically reasonable because the complex-valued fading parameter can be obtained via a channel estimator and the resulting estimate is Gaussian distributed [26, 27]. The estimation model is written for all l and k as

$$\hat{\alpha}_l^{(k)} = \alpha_l^{(k)} + w_l^{(k)} \quad (8)$$

where $w_l^{(k)}$ is the estimate noise in the l -th path for user k and it is assumed statistically independent complex-valued Gaussian variable with zero mean and variance $\sigma_{w_{lk}}^2$ for all l and k .

3 Multistage Interference Cancellation (MIC)

In this section, we first describe the output signals of the correlators. Then, we briefly review the conventional Rake combiner and the related MIC with full SI cancellation [1, 2]. Thereafter, we propose the new MIC, in which the MAI and the partial SI (the SII part) are reconstructed and subtracted from the received signal.

3.1 Correlation Output Signals

At the first part of any receiver under consideration, we assume that there are $\sum_{k=1}^K L_k$ correlators with the waveforms $\{a_k^*(t - \tau_l^{(k)}), l = 1, 2, \dots, L_k\}$ to generate the decision variables for K users, where the superscript “*” denotes the complex conjugate. For user u in the q -th fading path, the received signal $r(t)$ is correlated with $\{a_u^*(t - \tau_q^{(u)})\}$ and integrated from $nT_b + \tau_q^{(u)}$ to $(n+1)T_b + \tau_q^{(u)}$. Then, the output signal will be sampled at the time instant $(n+1)T_b + \tau_q^{(u)}$. The resulting sample, denoted by $V_{n,q}^{(u)}$, is given by

$$\begin{aligned} V_{n,q}^{(u)} &= \frac{1}{\sqrt{2N}} \int_{nT_b + \tau_q^{(u)}}^{(n+1)T_b + \tau_q^{(u)}} r(t) a_u^*(t - \tau_q^{(u)}) dt \\ &= \sum_{k=1}^K \sqrt{2\rho_k} \sum_{l=1}^{L_k} \alpha_l^{(k)} \left[e^{-j\phi_{n-m-1}^{(k)}} R_{k,u}(\tau_{k,l;u,q}^l) + e^{-j\phi_{n-m}^{(k)}} \hat{R}_{k,u}(\tau_{k,l;u,q}^l) \right] + \eta_{n,q}^{(u)} \end{aligned} \quad (9)$$

where $\frac{1}{\sqrt{2N}}$ is a normalization factor, T_c is set to 1 without loss of generality, $m := \lfloor (\tau_l^{(k)} - \tau_q^{(u)})/T_b \rfloor$, and $\tau_{k,l;u,q}^l := (\tau_l^{(k)} - \tau_q^{(u)}) - mT_b$. $R_{k,u}(\tau) = \frac{1}{2N} \int_0^T a_k(t - \tau) a_u^*(t) dt$ and $\hat{R}_{k,u}(\tau) = \frac{1}{2N} \int_{\tau}^{T_b} a_k(t - \tau) a_u^*(t) dt$ are the partial correlation functions as similarly defined in [28] but normalized by $1/2N$ and with complex-valued PN codes. Here, the carrier phase shifts have been absorbed into $\{\alpha_l^{(k)}\}$ as previously mentioned. $\eta_{n,q}^{(u)}$ is the noise component given by

$$\eta_{n,q}^{(u)} = \frac{1}{\sqrt{2N}} \int_{nT_b + \tau_q^{(u)}}^{(n+1)T_b + \tau_q^{(u)}} z(t) a_u^*(t - \tau_q^{(u)}) dt \quad (10)$$

Since $z(t)$ is the additive white Gaussian noise with zero mean and unit power spectral density, $\eta_{n,q}^{(u)}$ is also Gaussian with zero mean and unit variance. Due to the possible overlapped integration period, the noise components, $\{\eta_{n,q}^{(u)}\}$, could be correlated. The covariance of $\eta_{n_1,q_1}^{(u_1)}$ and $\eta_{n_2,q_2}^{(u_2)}$ is given by

$$\frac{1}{2} E \left\{ \eta_{n_1,q_1}^{(u_1)} [\eta_{n_2,q_2}^{(u_2)}]^* \right\} = \begin{cases} 0 & \text{if } \tau_1^L \leq \tau_2^S \text{ or } \tau_2^L \leq \tau_1^S \\ R_{u_2,u_1}(\tau_2^L - \tau_1^S) & \text{if } \tau_1^S < \tau_2^L \leq \tau_1^L \\ R_{u_1,u_2}^*(\tau_1^L - \tau_2^S) & \text{if } \tau_2^S < \tau_1^L \leq \tau_2^L \end{cases} \quad (11)$$

where $\tau_i^S = n_i T_b + \tau_{q_i}^{(u_i)}$ and $\tau_i^L = \tau_i^S + T_b$ for $i = 1, 2$.

It is noteworthy to mention that in (9), we made two assumptions, namely, the rectangular chip waveform for $P_{T_c}(t)$ and the perfect estimates of time delays $\{\tau_q^{(u)}\}$. In practice, the chip waveform other than the rectangular

one may be adopted. For arbitrary $P_{T_c}(t)$ if it is time-limited within $[0, T_c]$, the expression in (9) can be shown still valid (The involved partial correlation functions $R_{k,u}(\tau)$ and $\hat{R}_{k,u}(\tau)$ have to be re-evaluated relying on the adopted $P_{T_c}(t)$). If the duration of $P_{T_c}(t)$ exceeds T_c interval, the above expression is not accurate since there would be additional interferences created by the tails of the chip waveform. However, due to the fact that the tails can be designed to decay rapidly so as to reduce the possible interference [3], we can still use the above expression as an approximation. On the other hand, the imperfect estimates of time delays can degrade the system performance as shown in [29] for the Rake receiver. Later, in Section 5, we present several simulation results to show the effects of the imperfect time delay estimates on the performances of the MIC schemes.

3.2 Conventional Rake combiner

For the slowly time-varying channel, the fading parameters $\{\alpha_q^{(u)}\}$ can be estimated and the estimation model given by (8). To combat fading, the Rake-type combiner can be used to collect the signal replicas, i.e., $V_{n,q}^{(u)}$, over L_u paths. As a result, the combiner output in the Rake receiver is given by [3]

$$X_n^{(u)} = [\hat{\underline{\alpha}}^{(u)}]^H \underline{V}_n^{(u)} \quad (12)$$

where $[\cdot]^H$ denotes the Hermitian transpose of $[\cdot]$, $\underline{V}_n^{(u)} = [V_{n,1}^{(u)}, V_{n,2}^{(u)}, \dots, V_{n,L_u}^{(u)}]^T$ and $\hat{\underline{\alpha}}^{(u)} = [\hat{\alpha}_1^{(u)}, \hat{\alpha}_2^{(u)}, \dots, \hat{\alpha}_{L_u}^{(u)}]^T$, in which $[\cdot]^T$ denotes the transpose of $[\cdot]$.

After computing the following decision variables for QPSK,

$$D_p = \text{Re} \left\{ X_n^{(u)} e^{j\psi_p} \right\} \quad (13)$$

where $\psi_p := 2\pi(p-1)/4$, $p = 1, 2, \dots, 4$, the symbol is decided in favor of

$$\hat{\phi}_n^{(u)} = \psi_p = \text{argmax}_p \{ D_p \} \quad (14)$$

We can see that in the conventional Rake combiner, each user independently demodulates the received signal and then combines the replicas from multiple fading paths for symbol decision. In the detection, all other multiuser and multipath signals are treated as interference. Therefore, although the approach is quite simple, the performance of the Rake combiner is detrimentally affected by the interferences from multiple users and multiple paths. To improve the performance, multistage interference cancellation (MIC) [1, 2] algorithm can be applied.

3.3 Previous MIC with Full SI cancellation

To elaborate, we may rewrite $V_{n,q}^{(u)}$ of (9) into

$$V_{n,q}^{(u)} = \sqrt{2\rho_u} \alpha_q^{(u)} e^{-j\phi_n^{(u)}} + S c_{n,q}^{(u)} + S i_{n,q}^{(u)} + M_{n,q}^{(u)} + \eta_{n,q}^{(u)} \quad (15)$$

where $SC_{n,q}^{(u)}$, $Si_{n,q}^{(u)}$, and $M_{n,q}^{(u)}$ are respectively defined as

$$SC_{n,q}^{(u)} = \sqrt{2\rho_u} \sum_{l=1, l \neq q}^{L_u} \alpha_l^{(u)} e^{-j\phi_n^{(u)}} \ddot{R}_{u,u}(\tau'_{u,l;u,q}) \quad (16)$$

$$Si_{n,q}^{(u)} = \sqrt{2\rho_u} \sum_{l=1, l \neq q}^{L_u} \alpha_l^{(u)} \left[d_{m+1} e^{-j\phi_{n-m-1}^{(u)}} R_{u,u}(\tau'_{u,l;u,q}) + d_m e^{-j\phi_{n-m}^{(u)}} \hat{R}_{u,u}(\tau'_{u,l;u,q}) \right] \quad (17)$$

and

$$M_{n,q}^{(u)} = \sum_{k=1, k \neq u}^K \sqrt{2\rho_k} \sum_{l=1}^{L_k} \alpha_l^{(k)} \left[e^{-j\phi_{n-m-1}^{(k)}} R_{k,u}(\tau'_{k,l;u,q}) + e^{-j\phi_{n-m}^{(k)}} \hat{R}_{k,u}(\tau'_{k,l;u,q}) \right] \quad (18)$$

Here, $\ddot{R}_{u,u}(\tau)$ is set to either $R_{u,u}(\tau)$ or $\hat{R}_{u,u}(\tau)$ depending on $\tau_l^{(u)} < \tau_q^{(u)}$ or not. In (17), d_i is an index function and it is set to 0 if $i = 0$ and 1 otherwise. $S_{G_{n,q}}^{(u)}$ is the self current-symbol interference (SCI) and $S_{I_{n,q}}^{(u)}$ the self inter-symbol interference (SII). The sum of the SCI and the SII is the total self-interference (SI) for user u . $M_{n,q}^{(u)}$ is the multiple-access interference (MAI).

As shown in [1, 2], in each stage of the MIC, the MAI and the full SI (both the SII and the SCI) can be reconstructed and subtracted from the received signal before the symbol decision, and the resulting performance of the MIC can be much better than the conventional single-user receiver. Suppose that we are in the i -th stage and we have already obtained the tentative decisions in the previous stage for all interfering symbols. The output of the canceler can be given by

$$V_{n,q}^{(u)}(i) = V_{n,q}^{(u)} - \hat{S}C_{n,q}^{(u)}(i-1) - \hat{S}i_{n,q}^{(u)}(i-1) - \hat{M}_{n,q}^{(u)}(i-1) \quad (19)$$

where $\hat{S}C_{n,q}^{(u)}(i-1)$, $\hat{S}i_{n,q}^{(u)}(i-1)$, and $\hat{M}_{n,q}^{(u)}(i-1)$ are the reconstructed parts of $S_{G_{n,q}}^{(u)}$, $S_{I_{n,q}}^{(u)}$, and $M_{n,q}^{(u)}$, respectively. They can be calculated via (16), (17), and (18), respectively, by replacing $\{\hat{\phi}_n^{(k)}\}$ and $\{\hat{\alpha}_l^{(k)}\}$ with $\{\hat{\alpha}_l^{(k)}\}$ and $\{\hat{\phi}_n^{(k)}\}$. Here, $\hat{\alpha}_l^{(k)}$ denotes the channel estimate given by (8) and $\hat{\phi}_n^{(k)}(i-1)$ the tentative decision of $\phi_n^{(k)}$ in the $(i-1)$ -th stage for the n -th symbol and user k .

If the MAI and the SI can be successfully subtracted from $V_{n,q}^{(u)}(i)$ in (19), the resulting signal contains only the faded signal $\alpha_q^{(u)} \sqrt{2\rho_u} e^{-j\phi_n^{(u)}}$ and the noise component $\eta_n^{(u)}$ and there are no superimposed multipath signals. Thus, the Rake combining can be applied to collecting the signal replicas. The combiner output in the i -th stage can be given by

$$X_n^{(u)}(i) = [\hat{\underline{\alpha}}^{(u)}]^H \underline{V}_n^{(u)}(i) \quad (20)$$

where $\underline{V}_n^{(u)}(i) = [V_{n,1}^{(u)}(i), V_{n,2}^{(u)}(i), \dots, V_{n,L_u}^{(u)}(i)]^T$.

As discussed in the previous subsection, we can compute the following decision variable for QPSK,

$$D_p(i) = \text{Re} \left\{ X_n^{(u)}(i) e^{j\psi_p} \right\} \quad (21)$$

where $\psi_p := 2\pi(p-1)/4$, $p = 1, 2, \dots, 4$, and then make the symbol decision according to

$$\hat{\phi}_n^{(u)}(i) = \psi_p = \operatorname{argmax}_p \{D_p(i)\} \quad (22)$$

For the above MIC, we have to consider the tentative decisions in the initial stage, i.e., $i = 0$. For simplicity, we let $V_{n,q}^{(u)}(0) = V_{n,q}^{(u)}$. Based on $V_{n,q}^{(u)}(0)$, the tentative decision $\hat{\phi}_n^{(u)}(0)$ can be readily obtained by following (20) to (22). As such, the tentative decisions made in the initial stage are equivalent to those in the conventional Rake combiner.

In the above MIC with full SI cancellation (MIC-FSI), the SCI is regarded as an interference to be subtracted together with the SII and the MAI in (19). Nevertheless, the SCI contains the current symbol and it would be useful for symbol decision. As an illustration, we consider the received signal in the first arriving path $V_{n,1}^{(u)}(i)$ and suppose that in the i -th stage, all the MAI and the SII parts have been subtracted from the received signal such that

$$V_{n,1}^{(u)}(i) = \sqrt{2\rho_u} \alpha_1^{(u)} e^{-j\phi_n^{(u)}} + S_{n,1}^{(u)} + \eta_{n,1}^{(u)} \quad (23)$$

where $S_{n,1}^{(u)} = \sqrt{2\rho_u} \sum_{l=2}^{L_u} \alpha_l^{(u)} e^{-j\phi_n^{(u)}} \ddot{R}_{u,u}(\tau'_{u,l;u,1})$ is the SCI part, which also contains the current information data $\phi_n^{(u)}$.

Now, if we disregard the received signals from other paths and assume the perfect channel knowledge, the test statistic X for the optimum demodulation is not given by $[\alpha_1^{(u)}]^* \cdot V_{n,1}^{(u)}(i)$. Rather, it would be [3]

$$X = [\beta_1^{(u)}]^* \cdot V_{n,1}^{(u)}(i) = [\beta_1^{(u)}]^* \cdot \left[\beta_1^{(u)} e^{-j\phi_n^{(u)}} + \eta_{n,1}^{(u)} \right] \quad (24)$$

where $\beta_1^{(u)} := \sqrt{2\rho_u} \alpha_1^{(u)} + \sqrt{2\rho_u} \sum_{l=2}^{L_u} \alpha_l^{(u)} \ddot{R}_{u,u}(\tau'_{u,l;u,1})$.

By using (24), the SCI part in (23) is treated as a useful signal for symbol decision, rather than the interference in the SCI subtraction, so as to enhance the resulting performance. In the following, we modify the MIC so that in each stage, we only reconstruct $S_{n,q}^{(u)}$ and $M_{n,q}^{(u)}$ and then subtract them in the canceler.

3.4 New MIC with Partial SI Cancellation

In this subsection, we consider the MIC with the subtraction of the MAI and the partial SI (the SII part) rather than the total SI. The Rake combining is still equipped with the MIC to collect the fading replicas. We will show that after removing the MAI and the SII, further Rake combining can lead to an equivalent result to that obtained by the decorrelating approach for separating the multipath signals.

Suppose that we are now in the i -th stage and have already obtained the tentative decisions in the previous stage for all interfering symbols involved in $V_{n,q}^{(u)}$. The output of the canceler for user u is given by

$$V_{n,q}^{(u)}(i) = V_{n,q}^{(u)} - \hat{S}_{i,n,q}^{(u)}(i-1) - \hat{M}_{n,q}^{(u)}(i-1) \quad (25)$$

where as in the previous MIC-FSI, $\hat{S}_{n,q}^{(u)}(i-1)$ and $\hat{M}_{n,q}^{(u)}(i-1)$ are the reconstructed parts of $S_{n,q}^{(u)}$ and $M_{n,q}^{(u)}$, respectively.

Based on $V_{n,q}^{(u)}(i)$, the tentative symbol decision for $\phi_n^{(u)}$ follows (20)-(22). The tentative decisions in the initial stage ($i = 0$) are the same as in the MIC-FSI.

As an illustrative example, the structure of the new 2-stage MIC with the partial SI cancellation (MIC-PSI) is described in Fig. 3, where the reconstruction of the SII and the MAI parts is subtracted from the received sample and then the resulting replicas are combined for symbol decision. If the SCI part is added to the reconstruction and the subtraction, the structure can reflect the MIC with the full SI cancellation [1, 2] and the Rake combining. Besides, note that there is no interference cancellation for the combiner output $X_n^{(u)}(0)$ in the initial stage. Hence, $X_n^{(u)}(0)$ is identical to that in the conventional Rake receiver and it suggests that the performance of the 0-stage MIC is the same to that of the Rake receiver.

To gain insight of the MIC-PSI, we consider a special case by assuming that all the tentative decisions in the $(i-1)$ -th stage for interfering symbols are correct such that the SII part, $S_{h,q}^{(u)}$, and the MAI part, $M_{n,q}^{(u)}$, are totally removed. The resulting signal can be written as

$$\underline{V}_n^{(u)}(i) = \mathbf{R}_s \underline{\alpha}^{(u)} \sqrt{2\rho_u} e^{-j\phi_n^{(u)}} + \underline{\eta}_n^{(u)} \quad (26)$$

where $\underline{\eta}_n^{(u)} = [\eta_{n,1}^{(u)}, \eta_{n,2}^{(u)}, \dots, \eta_{n,L_u}^{(u)}]^T$.

\mathbf{R}_s in (26) is an $L_u \times L_u$ correlation matrix of the signature waveforms. More precisely, its ij -th entry, denoted by $(\mathbf{R}_s)_{ij}$, is set to $\hat{R}_{u,u}(\tau_j^{(u)} - \tau_i^{(u)})$ if $\tau_j^{(u)} \geq \tau_i^{(u)}$ and $R_{u,u}(T_b + \tau_j^{(u)} - \tau_i^{(u)})$ otherwise. For each user, the corresponding correlation matrix \mathbf{R}_s would be different. However, from the definitions of $R_{u,u}(\tau)$ and $\hat{R}_{u,u}(\tau)$ mentioned in (9), it can be shown that \mathbf{R}_s for any user is a Hermitian matrix, and all the diagonal elements are one. Moreover, by (11), the correlation matrix of $\underline{\eta}_n^{(u)}$ can be recognized to be \mathbf{R}_s .

It is well known that the decorrelating operation is very useful in separating the multiuser and multipath signals [18]. Similarly, by pre-multiplying (26) with \mathbf{R}_s inverse (\mathbf{R}_s^{-1}), the multipath signals can be separated. We have

$$U(i) = \mathbf{R}_s^{-1} \underline{V}_n^{(u)}(i) = \underline{\alpha}^{(u)} \sqrt{2\rho_u} e^{-j\phi_n^{(u)}} + \underline{w}_n^{(u)} \quad (27)$$

where $\underline{w}_n^{(u)} = \mathbf{R}_s^{-1} \underline{\eta}_n^{(u)}$ and $\frac{1}{2} E\{\underline{w}_n^{(u)} [\underline{w}_n^{(u)}]^H\} = \mathbf{R}_s^{-1}$.

The noise vector $\underline{w}_n^{(u)}$ in (27) is correlated and therefore noise whitening approach is usually applied in order to obtain the maximal ratio combining [3, 18]. For the correlation matrix \mathbf{R}_s , we let $\mathbf{R}_s = \mathbf{Q}_s \Lambda_s \mathbf{Q}_s^H$, where \mathbf{Q}_s is the orthogonal matrix and $\Lambda_s = \text{diag}(\lambda_1, \lambda_2, \dots, \lambda_{L_u})$ is the diagonal matrix, in which $\{\lambda_q, q = 1, 2, \dots, L_u\}$ are the eigenvalues of \mathbf{R}_s that are real and nonnegative [30]. Next, by pre-multiplying (27) with $\Lambda_s^{-\frac{1}{2}} \mathbf{Q}_s^H$ to

whiten the noise vector, the output of the Rake combiner is given by

$$\begin{aligned} X_n^{(u)}(i) &= \left[\Lambda_s^{\frac{1}{2}} \mathbf{Q}_s^H \hat{\underline{\alpha}}^{(u)} \right]^H \left[\Lambda_s^{\frac{1}{2}} \mathbf{Q}_s^H U(i) \right] \\ &= \left[\hat{\underline{\beta}}^{(u)} \right]^H \left[\underline{\beta}^{(u)} \sqrt{2\rho_u} e^{-j\phi_n^{(u)}} + \underline{\xi}_n^{(u)} \right] \end{aligned} \quad (28)$$

where $\underline{\beta}^{(u)} := \Lambda_s^{\frac{1}{2}} \mathbf{Q}_s^H \underline{\alpha}^{(u)}$, $\hat{\underline{\beta}}^{(u)} := \Lambda_s^{\frac{1}{2}} \mathbf{Q}_s^H \hat{\underline{\alpha}}^{(u)}$, and $\underline{\xi}_n^{(u)} := \Lambda_s^{\frac{1}{2}} \mathbf{Q}_s^H \underline{w}_n^{(u)} = \Lambda_s^{-\frac{1}{2}} \mathbf{Q}_s^H \underline{\eta}_n^{(u)}$.

The above equation implies that the samples over L_u paths in (26) can be transformed to the form of $\underline{\beta}^{(u)} \sqrt{2\rho_u} e^{-j\phi_n^{(u)}} + \underline{\xi}_n^{(u)}$ with statistically independent noise vector $\underline{\xi}_n^{(u)}$. Conditioning on $\underline{\beta}^{(u)}$, (28) is the optimum test statistic [3]. On the other hand, if we rewrite (28) and then use (27) and (26), we obtain

$$\begin{aligned} X_n^{(u)}(i) &= \left[\hat{\underline{\alpha}}^{(u)} \right]^H \mathbf{Q}_s \Lambda_s^{\frac{1}{2}} \left[\Lambda_s^{\frac{1}{2}} \mathbf{Q}_s^H U(i) \right] \\ &= \left[\hat{\underline{\alpha}}^{(u)} \right]^H \left[\mathbf{R}_s U(i) \right] \\ &= \left[\hat{\underline{\alpha}}^{(u)} \right]^H \underline{V}_n^{(u)}(i) \end{aligned} \quad (29)$$

The equivalence of (29) to (28) illustrates that if the SII and the MAI can be totally removed, the output of the Rake combiner is equivalent to that obtained by the decorrelating and noise-whitening approach. Here, the decorrelating operation under discussion is conducted over multiple fading paths for each user rather than for all users and paths. Hence, its complexity is much lower in comparison with the combined multiuser and multipath asynchronous decorrelator [18]. Furthermore, the above discussion shows that if the subtraction of the SII and the MAI is successful, there is no need to add an extra decorrelator because the Rake combining inherently includes the decorrelating operation to separate the multipath signals for each user and to further whiten the noise. In this sense, the complexity is further reduced. It also implies that the SCI in the introduced MIC-PSI is treated as a useful signal for test statistic rather than an interference.

4 Performance analysis

In this section, we evaluate the performance of the MIC-PSI in QPSK multiuser system over multipath Rayleigh fading channels. In the analysis, we adopt the similar approach developed by Kam [31] to express the bit error rate in the form of probabilities that the test statistic falls into the wrong decision and then we employ the characteristic function to evaluate the probability [18, 32, 33]. To provide a benchmark for system performance, we first consider an ideal single-user case by ignoring all the SII and MAI. Then, we derive the upper and lower bounds on the performance of the MIC-PSI in a multi-user environment.

In the following, the indexes n , u , and i of $X_n^{(u)}(i)$ are omitted whenever there is no ambiguity.

4.1 Ideal performance in single-user case

We assume that all the symbols are transmitted with equal probability. By ignoring the SII and MAI, the received signal is reduced to (26) and the output of the combiner, X , can be expressed in either (28) or (29).

Suppose that $\phi_n^{(u)} = \psi$ is transmitted. Conditioning on ψ , the symbol error rate for QPSK is given by [31]

$$P_s = \sum_{p=1}^3 A_p \quad (30)$$

where $A_p = \Pr\{X e^{j\psi} \in R_p | \psi\}$ is the conditional probability that $X e^{j\psi}$ falls into the decision region R_p .

Now, consider the combiner output X . Using (28), we have

$$X e^{j\psi} = [\hat{\underline{\beta}}^{(u)}]^H \left[\underline{\beta}^{(u)} \sqrt{2\rho_u} + \underline{\xi}_n^{(u)} e^{j\psi} \right] \quad (31)$$

Note that $\underline{\xi}_n^{(u)}$ is a Gaussian vector and together with the phase shift $e^{j\psi}$, $\underline{\xi}_n^{(u)} e^{j\psi}$ is still a Gaussian vector with zero mean and identity covariance matrix. It implies that the conditional probability $A_p = \Pr\{X e^{j\psi} \in R_p | \psi\}$ is irrelevant to ψ . Therefore, in the following, we set $\phi_n^{(u)} = \psi = 0$ without loss of generality.

Usually, it is meaningful to convert the symbol error rate to the bit error rate (BER). By employing the Gray code bit mapping, the BER is given by [31]

$$P_b = (A_1 + 2A_2 + A_3)/2 = \mathcal{F}(\gamma = -\pi/4) \quad (32)$$

where $\mathcal{F}(\gamma) := \Pr\{\text{Re}\{X e^{j\gamma}\} < 0\}$.

In computing $\mathcal{F}(\gamma)$, we adopt the characteristic function (CF) approach [18, 32, 33]. Letting $\Phi_\gamma(\omega)$ denote the CF of $\text{Re}\{X e^{j\gamma}\}$, we have

$$\mathcal{F}(\gamma) = - \sum_{\{\omega_p\}} \text{Res}[\Phi_\gamma(\omega)/\omega, \omega_p] \quad (33)$$

where $\{\omega_p\}$ denotes the set of poles of $\Phi_\gamma(\omega)/\omega$ in the upper half plane ($\text{Im}(\omega) > 0$) and $\text{Res}[f(\omega), \omega_p]$ the residue of $f(\omega)$ at $\omega = \omega_p$. Here, (33) is valid on the premise that $\Phi_\gamma(\omega)/\omega$ has at least a double zero at $\omega = \infty$ to allow the use of the residue theorem [32].

Next, we evaluate $\Phi_\gamma(\omega)$. Substituting (8) into (28) yields

$$X = [\underline{\beta}^{(u)} + \Lambda_s^{\frac{1}{2}} \mathbf{Q}_s^H \Delta \underline{\alpha}^{(u)}]^H [\underline{\beta}^{(u)} \sqrt{2\rho_u} + \underline{\xi}_n^{(u)}] \quad (34)$$

where $\Delta \underline{\alpha}^{(u)} = \hat{\underline{\alpha}}^{(u)} - \underline{\alpha}^{(u)}$ denotes the vector of the estimation error.

Let $\mathbf{R}_\beta = \frac{1}{2} E\{\underline{\beta}^{(u)} [\underline{\beta}^{(u)}]^H\}$. By diagonalizing $\mathbf{R}_\beta = \mathbf{Q}_\beta \Lambda_\beta \mathbf{Q}_\beta^H$, where \mathbf{Q}_β is the orthogonal matrix and $\Lambda_\beta = \text{diag}(\sigma_1^2, \sigma_2^2, \dots, \sigma_{L_u}^2)$, where $\{\sigma_q^2, q = 1, 2, \dots, L_u\}$ are the eigenvalues of \mathbf{R}_β , (34) can be written as

$$\begin{aligned} X &= [\mathbf{Q}_\beta^H \underline{\beta}^{(u)} + \mathbf{Q}_\beta^H \Lambda_s^{\frac{1}{2}} \mathbf{Q}_s^H \Delta \underline{\alpha}^{(u)}]^H [\mathbf{Q}_\beta^H \underline{\beta}^{(u)} \sqrt{2\rho_u} + \mathbf{Q}_\beta^H \underline{\xi}_n^{(u)}] \\ &= [C + G]^H [C \sqrt{2\rho_u} + Z] \\ &= C^H C \sqrt{2\rho_u} + C^H (G \sqrt{2\rho_u} + Z) + G^H Z \end{aligned} \quad (35)$$

where $C := \mathbf{Q}_\beta^H \underline{\beta}^{(u)}$, $G := \mathbf{Q}_\beta^H \Lambda_s^{\frac{1}{2}} \mathbf{Q}_s^H \Delta \underline{\alpha}^{(u)}$ and $Z := \mathbf{Q}_\beta^H \underline{\xi}^{(u)}$.

The elements in the vector C are statistically independent, so are those in the vector Z . However, the elements in G may be correlated. We hence have

$$\frac{1}{2} E\{GG^H\} = \mathbf{Q}_\beta^H \Lambda_s^{\frac{1}{2}} \mathbf{Q}_s^H \frac{1}{2} E\{[\Delta \underline{\alpha}^{(u)}][\Delta \underline{\alpha}^{(u)}]^H\} \mathbf{Q}_s \Lambda_s^{\frac{1}{2}} \mathbf{Q}_\beta \quad (36)$$

In evaluating the CF of $\text{Re}\{X e^{j\gamma}\}$, we first assume $\frac{1}{2} E\{GG^H\} = \lambda^{(G)} \mathbf{I}$. As shown in Appendix A, the CF of $\text{Re}\{X e^{j\gamma}\}$ can be given by

$$\Phi_\gamma(\omega) = \prod_{q=1}^{L_u} \frac{1}{a_q^2 \omega^2 - 2j\omega b_q + 1} \quad (37)$$

where $a_q := \sqrt{[\lambda^{(Z)} + 2\rho_u \lambda^{(G)}] \sigma_q^2 + \lambda^{(Z)} \lambda^{(G)}}$ and $b_q := \sqrt{2\rho_u} \cos \gamma \sigma_q^2$.

In (37), $\lambda^{(Z)}$ actually can be set to 1 because we have already normalized the noise vector Z . Here, we still use $\lambda^{(Z)}$ instead of 1 so that (37) can be readily extended to the multi-user case as will be shown later.

With $\Phi_\gamma(\omega)$, the bit error rate can be readily obtained via (32) and (33). Here, for the purpose of further reference, we express the BER as the function of $\lambda^{(G)}$ and $\lambda^{(Z)}$, i.e.,

$$P_b(\lambda^{(G)}, \lambda^{(Z)}) = - \sum_{\{\omega_p\}} \text{Res} [\Phi_{\gamma=-\pi/4}(\omega)/\omega, \omega_p] \quad (38)$$

In general, the explicit expression of $\mathcal{F}(\gamma)$ depends on the order of the poles and is very complicated. If all the poles of $\Phi_\gamma(\omega)$ are distinct, it follows from (38) that

$$P_b(\lambda^{(G)}, \lambda^{(Z)}) = \sum_{q=1}^{L_u} \pi_q \frac{1}{2} \left[1 - \sqrt{\frac{b_q^2/a_q^2}{1 + b_q^2/a_q^2}} \right] \quad (39)$$

where

$$\pi_q = \prod_{l=1, l \neq q}^{L_u} \frac{1}{a_l^2 \omega^2 - 2j\omega b_l + 1} \Big|_{\omega=j(b_q/a_q + \sqrt{1+b_q^2/a_q^2})/a_q} \quad (40)$$

with $a_q := \sqrt{[\lambda^{(Z)} + 2\rho_u \lambda^{(G)}] \sigma_q^2 + \lambda^{(Z)} \lambda^{(G)}}$ and $b_q := \sqrt{2\rho_u} \sigma_q^2$.

The above BER expression is valid for both perfect and imperfect channel knowledge. In the case of perfect channel knowledge, one can readily check that by setting $\lambda^{(G)} = 0$ and $\lambda^{(Z)} = 1$, (39) simply reduces to Equation (14-5-28) of [3].

Now, we consider the correlated G . Due to the correlation of G and noise term $G^H Z$ in (35), to evaluate the CF of $\text{Re}\{X e^{j\gamma}\}$ is quite difficult. In the following, we attempt to derive the upper and lower bounds on the BER. Note that at SNR values of practical interest, the term $G^H Z$ is relatively small in comparison with the noise term $C^H (G \sqrt{2\rho_u} + Z)$ [3, page 275] and can be ignored. Hence, the upper and lower bounds on the BER are mainly corresponding to the maximum and minimum variances of the noise $C^H G \sqrt{2\rho_u}$, respectively. Note

here that conditioning on C , we have $\lambda_{min}^{(G)} C^H C \leq C^H \frac{1}{2} E\{GG^H\} C \leq \lambda_{max}^{(G)} C^H C$, where $\lambda_{max}^{(G)}$ and $\lambda_{min}^{(G)}$ are the maximum and minimum eigenvalues of the covariance matrix $\frac{1}{2} E\{GG^H\}$, respectively. Therefore, the upper and lower bounds on the BER can be obtained from (38) by setting $\frac{1}{2} E\{GG^H\}$ to $\lambda_{max}^{(G)} \mathbf{I}$ and $\lambda_{min}^{(G)} \mathbf{I}$, respectively. Specifically, we have

$$P_b^{(up)} = P_b(\lambda_{max}^{(G)}, 1) \quad (41)$$

$$P_b^{(low)} = P_b(\lambda_{min}^{(G)}, 1) \quad (42)$$

where $P_b(\lambda^{(G)}, \lambda^{(Z)})$ is the function defined in (38) and $\lambda^{(Z)}$ is now set to 1 because the noise vector has already been normalized. The superscripts (up) and (low) denote the upper and lower bounds, respectively. When the CF of $\text{Re}\{X e^{j\gamma}\}$ has L_u distinct poles, $P_b(\lambda^{(G)}, \lambda^{(Z)})$ can be evaluated via (39).

In order to evaluate the performance of a given user, we first need to compute the corresponding values for $\{\mathbf{R}_s, \lambda_{max}^{(G)}, \lambda_{min}^{(G)}\}$ and then adopt (41) and (42) to obtain the performance bounds. In the case of perfect channel knowledge, $\lambda_{max}^{(G)}$ and $\lambda_{min}^{(G)}$ can be set to 0, resulting in identical $P_b^{(up)}$ and $P_b^{(low)}$ which represent the exact expression for the probability of bit error in an ideal single-user system (i.e., the ISI is ignored).

4.2 Performance in multi-user system

4.2.1 Performance in the initial stage

We first consider the multi-user performance in the initial stage ($i = 0$). In the analysis, we assume that the interference terms, $S_{i_n, q}^{(u)}$ and $M_{n, q}^{(u)}$, are approximately Gaussian distributed for large K and $\{L_k\}$. Such approximation can provide good results, although it is not exactly correct [1, 2]. Therefore, the analysis here is similar to those in [1, 2] but with QPSK spreading and diversity effect.

We still assume that $\phi_n^{(u)} = 0$ is transmitted. The received signal in the initial stage is given by

$$\underline{V}_n^{(u)}(0) = \mathbf{R}_s \underline{\alpha}^{(u)} \sqrt{2\rho_u} + \underline{S}_{i_n}^{(u)} + \underline{M}_n^{(u)} + \underline{\eta}_n^{(u)} \quad (43)$$

where $\underline{S}_{i_n}^{(u)} := [S_{i_n, 1}^{(u)}, S_{i_n, 2}^{(u)}, \dots, S_{i_n, L_u}^{(u)}]^T$ and $\underline{M}_n^{(u)} := [M_{n, 1}^{(u)}, M_{n, 2}^{(u)}, \dots, M_{n, L_u}^{(u)}]^T$.

Similarly as in (35), the combiner output $X(0)$ can be written as

$$\begin{aligned} X(0) &= [\hat{\underline{\alpha}}^{(u)}]^H \underline{V}_n^{(u)}(0) \\ &= [\mathbf{Q}_\beta^H \hat{\underline{\beta}}^{(u)}]^H [\mathbf{Q}_\beta^H \underline{\beta}^{(u)} \sqrt{2\rho_u} + F(0) + \mathbf{Q}_\beta^H \underline{\xi}_n^{(u)}] \\ &= [C + G]^H [C \sqrt{2\rho_u} + F(0) + Z] \end{aligned} \quad (44)$$

where \mathbf{Q}_β is the orthogonal matrix which diagonalizes \mathbf{R}_β as previously mentioned, and $F(0) := \mathbf{Q}_\beta^H \Lambda_s^{-\frac{1}{2}} \mathbf{Q}_s^H (\underline{S}_{i_n}^{(u)} + \underline{M}_n^{(u)})$ denotes the interference term in $X(0)$.

The covariance matrix of G , denoted by \mathbf{R}_G , is given by (36), while the covariance matrix of $F(0)$, denoted by $\mathbf{R}_F(0)$, is evaluated in Appendix B. As in the previous subsection, at SNR values of practical interest, we can ignore the term $G^H[F(0) + Z]$. Therefore, the BER is mainly determined by the noise terms $G^H C \sqrt{2\rho_u}$ and $C^H[F(0) + Z]$. Now, let $\lambda_{max}^{(F)}(0)$ and $\lambda_{min}^{(F)}(0)$ denote the maximum and minimum eigenvalues of $\mathbf{R}_F(0)$, respectively. In deriving the upper bound for the BER, we may set $\frac{1}{2}E\{GG^H\} = \lambda_{max}^{(G)}\mathbf{I}$ and $\frac{1}{2}E\{F(0)F^H(0)\} = \lambda_{max}^{(F)}(0)\mathbf{I}$, while in deriving the lower bound for the BER, we may set $\frac{1}{2}E\{GG^H\} = \lambda_{min}^{(G)}\mathbf{I}$ and $\frac{1}{2}E\{F(0)F^H(0)\} = \lambda_{min}^{(F)}(0)\mathbf{I}$. As a result, the upper and lower bounds on the BER in the initial stage are respectively given by

$$P_b^{(up)}(0) = P_b(\lambda_{max}^{(G)}, 1 + \lambda_{max}^{(F)}(0)) \quad (45)$$

$$P_b^{(low)}(0) = P_b(\lambda_{min}^{(G)}, 1 + \lambda_{min}^{(F)}(0)) \quad (46)$$

where $P_b(\cdot, \cdot)$ can be evaluated via (38), of which the involved parameter a_q is computed using the arguments in $P_b(\cdot, \cdot)$.

Although not specified above, \mathbf{R}_G and $\mathbf{R}_F(0)$ are corresponding to the user of interest.

4.2.2 Performance in the i -th stage ($i > 0$)

Due to the subtraction of the interference part, the calculation of the interference covariance matrix in the i -th stage ($i > 0$) is slightly different from that in the initial stage.

Assume $\phi_n^{(u)} = 0$. The output signal of the cancellation in the i -th stage is given by

$$\underline{V}_n^{(u)}(i) = \mathbf{R}_s \underline{\alpha}^{(u)} \sqrt{2\rho_u} + \underline{\tilde{S}}_n^{(u)}(i-1) + \underline{\tilde{M}}_n^{(u)}(i-1) + \underline{\eta}_n^{(u)} \quad (47)$$

where

$$\underline{\tilde{S}}_n^{(u)}(i-1) = [\tilde{S}_{i_{n,1}}^{(u)}(i-1), \tilde{S}_{i_{n,2}}^{(u)}(i-1), \dots, \tilde{S}_{i_{n,L_u}}^{(u)}(i-1)]^T,$$

$$\underline{\tilde{M}}_n^{(u)}(i-1) = [\tilde{M}_{n,1}^{(u)}(i-1), \tilde{M}_{n,2}^{(u)}(i-1), \dots, \tilde{M}_{n,L_u}^{(u)}(i-1)]^T,$$

$$\tilde{S}_{i_{n,q}}^{(u)}(i-1) := S_{i_{n,q}}^{(u)} - \hat{S}_{i_{n,q}}^{(u)}(i-1), \text{ and } \tilde{M}_{n,q}^{(u)}(i-1) := M_{n,q}^{(u)} - \hat{M}_{n,q}^{(u)}(i-1).$$

It can be seen that in each stage, the test statistics for all users are correlated. Therefore, the tentative decisions for all interfering symbols in the $(i-1)$ -th stage, namely $\{\hat{\phi}_n^{(k)}(i-1)\}$, are also correlated and dependent on the fading parameters $\{\alpha_q^{(k)}\}$ and the noise components $\{\eta_{m,q}^{(k)}\}$. The performance evaluation in the i -th stage ($i > 0$) becomes more complicated. One possible approach is to compute the bit error rate conditioned on all $\{\alpha_q^{(k)}\}$ and then take the ensemble average [33]. However, this requires an excessive computational effort especially in evaluating the multiple-dimension numerical integration. With the well-designed PN codes, we can assume that $\{\hat{\phi}_n^{(k)}(i-1)\}$ are weakly correlated and the residual interference is approximately Gaussian distributed as in [1, 2]. Accordingly, following the approach in the initial stage, the

upper and lower bounds on the BER can be evaluated by relying on the covariance matrix of the interference vector $F(i) := \mathbf{Q}_\beta^H \Lambda_s^{-\frac{1}{2}} \mathbf{Q}_s^H [\underline{\tilde{S}}_n^{(u)}(i-1) + \underline{\tilde{M}}_n^{(u)}(i-1)]$.

Let $\mathbf{R}_F(i)$ denote the covariance matrix of $F(i)$. The evaluation of $\mathbf{R}_F(i)$ depends on the bit error rate in the previous stage ($i-1$), of which the exact result is unfortunately difficult to obtain. Therefore, we further let $\mathbf{R}_F^{(up)}(i)$ and $\mathbf{R}_F^{(low)}(i)$ denote the covariance matrix of $F(i)$ evaluated from $P_b^{(up)}(i-1)$ and $P_b^{(low)}(i-1)$, respectively. In Appendix C, the evaluation of $\mathbf{R}_F^{(up)}(i)$ and $\mathbf{R}_F^{(low)}(i)$ is given. For different users, the corresponding $P_b^{(up)}(i-1)$ and $P_b^{(low)}(i-1)$ are different. Therefore, in order to evaluate $\mathbf{R}_F^{(up)}(i)$ and $\mathbf{R}_F^{(low)}(i)$, all $P_b^{(up)}(i-1)$ and $P_b^{(low)}(i-1)$ for interfering users involved in $F(i)$ have to be evaluated.

Next, let $\lambda_{max}^{(F, up)}(i)$ denote the maximum eigenvalue of $\mathbf{R}_F^{(up)}(i)$ and $\lambda_{min}^{(F, low)}(i)$ the minimum eigenvalue of $\mathbf{R}_F^{(low)}(i)$. We can set $\frac{1}{2}E\{F(i)F^H(i)\}$ to $\lambda_{max}^{(F, up)}(i)\mathbf{I}$ and $\lambda_{min}^{(F, low)}(i)\mathbf{I}$, respectively, in computing the upper and lower bounds on the BER in the i -th stage. It then follows that

$$P_b^{(up)}(i) = P_b(\lambda_{max}^{(G)}, 1 + \lambda_{max}^{(F, up)}(i)) \quad (48)$$

$$P_b^{(low)}(i) = P_b(\lambda_{min}^{(G)}, 1 + \lambda_{min}^{(F, low)}(i)) \quad (49)$$

where $P_b(\cdot, \cdot)$ is evaluated via (38) as previously mentioned.

Once again, before applying (48) and (49) to evaluating the performance bounds for a particular user, we have to evaluate the corresponding \mathbf{R}_G , $\mathbf{R}_F^{(up)}(i)$, and $\mathbf{R}_F^{(low)}(i)$.

5 Analytical and Simulation Results

In this section, we present several analytical and simulation results for the BER of the MIC with partial SI cancellation (MIC-PSI) in QPSK asynchronous CDMA system over multipath Rayleigh fading channels. Without loss of generality, we consider the first user. For comparison, the BERs of the conventional Rake receiver and the previous MIC with full SI cancellation (MIC-FSI) are also presented.

5.1 System model

In the study, we consider an identical fade in all paths by setting $E\{[\alpha_l^{(k)}]^2\} = 2$, for which $\mathbf{R}_\alpha = \mathbf{I}$. The analysis is valid for arbitrary \mathbf{R}_α and applicable to unbalanced fading channels. For user k , the total SNR per bit over the L_k fading channels is set to $\frac{1}{2}L_k 2\rho_k E\{[\alpha_l^{(k)}]^2\}/\log_2 M = \rho_k L_k$, where $\log_2 M$ for M-PSK is a factor used to obtain the SNR per bit. The number of paths, L_k , is assumed to be the same for all users and denoted by L . Gold sequences with $N = 31$ are considered as the PN codes, where the m -sequences for generating Gold sequences are represented in octal by 45 (11001) and 67 (00011). Here the sequences in the brackets are the corresponding initial AO/LSE loadings [34]. For user k , the time delay associated with the

fading path, $t_l^{(k)}$, is set to $lT_c/2$, while the time delay associated with user k , $T^{(k)}$, is set to $(k-1)T_b/10 \bmod T_b$. The total time delay for user k in the l -th path is $\tau_l^{(k)} = T^{(k)} + lT_c/2$.

In the simulation, we need to generate the received samples $V_{n,q}^{(u)}$, the fading parameters, and the Gaussian noise components $\{r_{n,q}^{(u)}\}$ in (9) for $q = 1, 2, \dots, L$ and $u = 1, 2, \dots, K$. Due to the possible correlation between the noise components as shown in (11), we proceed the simulation trials as follows. In each trial, we generate a sequence of received samples $V_{n,q}^{(u)}$ for $q = 1, 2, \dots, L$ and $u = 1, 2, \dots, K$ from $n = n_o$ to $n = n_o + P - 1$, where P is the sequence length and n_o is a particular starting index. During the period from $n = n_o$ to $n = n_o + P - 1$, the correlation matrix of the noise components can be computed via (11) and denoted by \mathbf{R}_η . The correlated noise components $\{r_{n,q}^{(u)}\}$ are generated by multiplying the square-root matrix of \mathbf{R}_η with a sequence of white Gaussian noise samples. On the other hand, to represent the Rayleigh fading channel, the fading parameters of all users over L fading paths are randomly generated from sequence to sequence such that their amplitudes are Rayleigh-distributed. Within each period from $n = n_o$ to $n = n_o + P - 1$, however, the fading parameters remain unchanged.

The selection of the sequence length P is based on the number of stages in the MIC due to the partial inter-symbol interference. Specifically, in making the current symbol decision for a particular user, the MIC may have to estimate the tentative decisions in the previous stage for the two consecutive interfering symbols of other users (see (25) and Fig. 3). In other words, if the symbol decision in the S -stage of the MIC is considered, the number of involved interfering symbols in the initial stage would be at least $2S$. Here, in the simulation, the sequence length P is set to $2S + 3$ to make sure all the involved symbols are taken into consideration. In the S -stage MIC, the symbol decision will be made for the $(S + 1)$ -th symbol of this sequence. Since we wish to evaluate the performance of the MIC in the second stage, S is set to 2 through all the following simulations.

In this paper, instead of introducing a threshold for the soft decision as in [2], we focus on the hard decision in the MIC due to the fact that the determination of the optimum threshold is practically complicated. The analytical bounds on the BER can be evaluated using the formulae presented in the previous section, while the simulation results on BER are estimated from 3×10^6 Monte Carlo trials.

For notational simplicity, we use MIC-FSI- i and MIC-PSI- i to denote the i -stage MIC-FSI and MIC-PSI, respectively. In the initial stage, the MIC schemes (MIC-0) have the same performance as the conventional Rake receiver since there is no interference cancellation.

5.2 Illustrative Results

5.2.1 Case of perfect channel knowledge

We first consider the performance in the case of perfect channel knowledge. In the theoretical analysis, we set $\lambda^{(G)} = 0$.

The BERs for the MIC schemes in a 3-user system over a 2-path Rayleigh fading channel versus SNR are plotted in Fig. 4. All users are with equal power. The performance in a single-user environment is evaluated via (41) with $\lambda_{max}^{(G)} = 0$. The upper and lower bounds for the MIC-0 are evaluated via (45) and (46), respectively. The upper bounds for the MIC-PSI-1,2 are obtained by (48), while the corresponding lower bounds are very close to the performance in a single-user environment and not plotted for this reason. In the evaluation, \mathbf{R}_i is set to zero due to the perfect channel knowledge. The other BER points are obtained from the simulation. From the figure, it can be seen that both the MIC-PSI and the MIC-FSI with $i > 0$ can provide a significant performance improvement over the conventional Rake receiver (MIC-0), in which no interference cancellation scheme is used. In addition, the MIC-PSI-1 (partial SI cancellation) can provide an improvement in SNR of about 3dB at a BER of 10^{-4} , as compared to the MIC-FSI-1 (full SI cancellation). The results also indicate that the MIC-PSI offers a performance in a 3-user, frequency-selective, 2-path Rayleigh fading environment similar to that in a single-user case. Moreover, the upper bound is tight for low SNR values but looser for high SNR ones, especially in the case of the MIC-PSI-1. This can be explained as follows. From (48), where $\lambda_{max}^{(G)}$ is set to 0 because of the perfect channel knowledge, we note that given ρ_i and σ_q^2 , the maximum eigenvalue of the covariance matrix of the residual interference, i.e., $\lambda_{max}^{(F,up)}(i)$, mainly determines the upper bound. As shown in Appendix C, in computing the covariance matrix, we adopt the worst-case BER in the previous stage (MIC-0). That may result in some performance gap. In addition, for high SNR values, the interference part can be effectively removed such that the residual interference may not be well approximated by the Gaussian distribution. Hence, when the Gaussian approximation is adopted in the analysis, the analytical results may deviate from the simulation ones.

The effect of the number of users is studied next. The simulation results on the BER of the MIC schemes versus the number of users (K) at SNR= 20dB over a 2-path Rayleigh fading channel are plotted in Fig. 5 and compared with the analytical upper and lower bounds, evaluated by (45) and (46) for the MIC-0 and (48) and (49) for the MIC-PSI-1,2, respectively. All users are equal in power. It can be seen that as K increases, the performance of both the MIC-PSI-1 and MIC-FSI-1 is degraded. To improve the performance, the 2-stage MIC appears necessary, especially when K is large ($K > 7$). Besides, it is shown that the MIC-PSI outperforms the MIC-FSI. For example, the system using the MIC-PSI-2 can achieve a BER of 10^{-4} for 12 users or more while the MIC-FSI-2 cannot. Furthermore, it is shown that the simulation results are well bounded by the analytical bounds. In other words, the upper and lower bounds can be used for estimating the performance.

Fig. 6 shows the simulation results on the BER of the MIC in the case of unequal-power users. A system with 3 users over a 2-path fading channel is assumed. SNR# i is the SNR of user # i . The SNR#1 is set to 20dB while the SNR#3 varies relatively to SNR#1 as shown in the horizontal axis and SNR#2 is set to (SNR#3+SNR#1)/2 (in dB). The performance of the MIC-PSI-1,2 is much better than that of the MIC-0 due

to the cancellation of the MAI and SII and it is less susceptible to the values of SNR#3-SNR#2 than that of the MIC-0. However, the performance of the MIC-FSI-1,2 is slightly degraded as SNR#3 and SNR#2 become large. A possible explanation is that as SNR#3 and SNR#2 become large, the probability of making a wrong tentative decision for user #1 would increase and thus when the MIC-FSI subtracts the SCI part, which involves the tentative decision of user #1, the performance degradation will occur. It appears that the subtraction of the SCI in the MIC-FSI-1,2 cannot improve but worsen the performance. In contrast, the performance of the MIC-PSI-1,2 is almost insensitive to the power difference in the users. In other words, the MIC with the partial SI cancellation can tolerate more imperfection in power control.

In Fig. 7, the analytical and simulation results on the BER of the MIC schemes versus the number of diversities ($L = 1, 2, 3, 4$) in a 3-user system at SNR= 20dB and $N = 31$ over multipath Rayleigh fading channels are plotted, where L is also the number of fading paths. It is assumed that the receiver knows the number of paths so that L diversities can be applied to the case of L paths. All users have an equal power. In the case of $L = 1$ (i.e., no self interference), there is no difference in performance between the MIC-PSI and MIC-FSI because these two schemes are the same when there is no self interference. As L increases, the MIC-PSI-1 provides a significant performance improvement over the MIC-FSI-1 and the conventional Rake (MIC-0). This can be explained by the fact that the MIC-PSI-1 treats the self current interference (SCI) as the signal while the MIC-FSI-1 regards it as the interference. We also note that the simulation results of the MIC-PSI-1 are well bounded by the analytical results. The analytical bounds in case of MIC-0 become looser for large L because there would be more self interference in the initial stage. Note that for $L = 1$, the upper and lower bounds are merged together and represent the approximated BER for the MIC under the Gaussian approximation.

5.2.2 Effects of imperfect channel knowledge

We assume that the variance of the channel estimation error in (8) is the same for all l and k and can be denoted by σ_w^2 .

The simulation results on the BER versus σ_w^2 for the MIC schemes in a 3-user system with SNR=20dB and $N=31$ over a 2-path Rayleigh fading channel are plotted in Fig. 8, and compared with the analytical upper and lower bounds. The upper and lower bounds for the MIC-0 are evaluated by (45) and (46), respectively, while those for the MIC-1,2 are obtained by (48) and (49), respectively. All users are considered to have an equal power. It can be seen that when the variance of the channel estimation error is less than 10^{-2} , both the MIC-PSI and the MIC-FSI with $i > 0$ can provide a significant performance improvement over the conventional Rake receiver (MIC-0). As the variance of the estimation error increases, the performance improvement becomes smaller. Nevertheless, it is shown in Fig. 8 that even in the presence of the estimation error the MIC-PSI still

outperforms the previous one (MIC-FSI).

Further analytical and simulation results on the BER of the MIC schemes versus the number of users (K) at SNR=20dB over a 2-path Rayleigh fading channel are plotted in Fig. 9. The variance of the channel estimation error (σ_w^2) is set to 10^{-2} and all users are assumed to have an equal power. It can be seen that as K increases, the performances of both the MIC-PSI-1 and MIC-FSI-1 are degraded. Furthermore, the results show that in the case of imperfect channel knowledge, the MIC-PSI still performs better than the MIC-FSI. For example, to achieve a BER of 10^{-3} or better, the MIC-FSI-1,2 can only accommodate 7 and 9 active users, respectively, while the system can tolerate 9 active users in the MIC-PSI-1 and at least 12 users in the MIC-PSI-2. Once again, the simulation results are shown to be well bounded by analytical upper and lower bounds.

5.2.3 Effects of imperfect channel knowledge and time delay estimation

As mentioned earlier, we assume the perfect estimates of the time delays in this paper to simplify our analysis. This section presents simulation results on the BER performance of the MIC schemes in the presence of time delay estimation error. The time delay estimates can be given by

$$\hat{\tau}_l^{(k)} = \tau_l^{(k)} + \Delta\tau_l^{(k)}$$

where $\hat{\tau}_l^{(k)}$ is the estimate of the time delay in the l -th path for user k and $\Delta\tau_l^{(k)}$ the estimation error.

In the simulation, we replace all time delays $\{\tau_l^{(k)}\}$ with $\{\hat{\tau}_l^{(k)}\}$ for the noise correlation and the reconstruction of the interferences except those in $V_{n,q}^{(u)}$ of (9), for which the replacement is $m := \lfloor (\tau_l^{(k)} - \hat{\tau}_q^{(u)})/T_b \rfloor$ together with $\tau'_{k,l;u,q} := (\tau_l^{(k)} - \hat{\tau}_q^{(u)}) - mT_b$. In [29], $\Delta\tau_l^{(k)}$ was modeled as a zero mean Gaussian random variable. Here, we assume $\Delta\tau_l^{(k)}$ is deterministic and the same for all l and k and thus can be denoted by $\Delta\tau$. This assumption is unrealistic but greatly simplifies our simulation and the results could be useful to assess the effect of the random variable $\Delta\tau_l^{(k)}$. Otherwise, the aforementioned noise correlation matrix \mathbf{R}_η , computed from the time delay estimates $\hat{\tau}_l^{(k)}$, has to be calculated and diagonalized in each trial.

The simulation results on the BER performance of the MIC schemes in 3 and 8-user systems over a 2-path Rayleigh fading channel are plotted in Fig. 10, where SNR=20dB, $N=31$, and $\sigma_w^2 = 10^{-2}$. The results show that when the time delay $\Delta\tau$ is less than 10^{-2} , there is no significant performance degradation for all the MIC schemes, while as $\Delta\tau$ increases especially when $\Delta\tau \geq 10^{-1}$, the performance is seriously deteriorated. In addition, the MIC-PSI-1,2 conduct better than the MIC-FSI-1,2 in the presence of the time delay estimation error. Furthermore, although the deterministic $\Delta\tau$ is considered in the figure to show its effect on the BER, the results also suggest that for a random variable $\Delta\tau_l^{(k)}$, if the probability of $\Delta\tau_l^{(k)} \geq 10^{-2}$ is very small, there would be no significant performance degradation on the MIC schemes.

6 Conclusions

This paper shows that the multistage interference cancellation (MIC) using the partial SI cancellation in conjunction with the Rake combining can provide a satisfactory performance in a QPSK asynchronous DS/CDMA system over multipath fading channels. By removing only the self inter-symbol interference rather than the total SI, the introduced MIC-PSI outperforms the previously proposed MIC-FSI and has a performance close to that in the single-user system. The paper also presents a derivation of the bit error probability taking into consideration the effects of the diversity combining, noise correlation among the fading replicas, and channel estimation error. Analysis and simulation indicate that in the presence of channel estimation errors, performance degradation occurs in both the MIC-PSI and MIC-FSI. However, the introduced MIC-PSI still provides a better performance than the MIC-FSI.

Acknowledgment

This work is partially supported by Ericsson Research Canada. The authors are grateful to the reviewers and editors and acknowledge with pleasure their constructive comments.

Appendix

A Evaluation of the CF of $\text{Re}\{X e^{j\gamma}\}$ in (37)

From (35), $\text{Re}\{X e^{j\gamma}\}$ can be written as

$$\text{Re}\{X e^{j\gamma}\} = \frac{1}{2} \sum_{q=1}^{L_u} \{Y_{1,q}^* Y_{2,q} + Y_{1,q} Y_{2,q}^*\} \quad (50)$$

where $Y_{1,q} = c_q + g_q$ and $Y_{2,q} = (c_q \sqrt{2\rho_u} + z_q) e^{j\gamma}$, of which c_q , g_q , and z_q are the q -th elements in the vectors C , G , and Z , respectively.

We assume that $\frac{1}{2} E\{GG^H\} = \lambda^{(G)} \mathbf{I}$. Thus, conditioning on the channel parameter vector C , $Y_{1,q}$ and $Y_{2,q}$ form a pair of complex-valued Gaussian random variables. For different q , they are statistically independent but the pairs of $\{Y_{1,q}, Y_{2,q}\}$ may not be identically distributed. If they were, the results in [3, Appendix C] for the error probability in the presence of the estimation error could be directly applied.

By eq.B-5 of [3], the CF of $\text{Re}\{X e^{j\gamma}\}$ conditioned on $\{c_q\}$, denoted by $\Phi_\gamma(\omega|C)$, can be written as

$$\Phi_\gamma(\omega|C) = \prod_{q=1}^{L_u} \frac{\mu^2}{\omega^2 + \mu^2} \exp \left\{ \frac{\mu^2}{\omega^2 + \mu^2} \left[-\frac{\omega^2}{2} (\lambda^{(Z)} + 2\rho_u \lambda^{(G)}) + j\omega \sqrt{2\rho_u} \cos \gamma \right] |c_q|^2 \right\} \quad (51)$$

where $\lambda^{(Z)}$ and $\lambda^{(G)}$ are the variances of z_q and g_q , respectively, and $\mu=1/\sqrt{\lambda^{(Z)}\lambda^{(G)}}$.

In (51), c_q is Gaussian distributed with zero mean and variance σ_q^2 . Thus, $|c_q|^2$ is Rayleigh distributed. Averaging $\Phi_\gamma(\omega|C)$ over $\{|c_q|^2, q = 1, 2, \dots, L_u\}$, it yields $\Phi_\gamma(\omega)$ as shown in (37).

B Evaluation of $\mathbf{R}_F(0)$

In the text, we use $\mathbf{R}_F(0)$ to denote the covariance matrix of $F(0) = \mathbf{Q}_\beta^H \Lambda_s^{-\frac{1}{2}} \mathbf{Q}_s^H [\underline{S}_n^{(u)} + \underline{M}_n^{(u)}]$. We have

$$\mathbf{R}_F(0) = \mathbf{Q}_\beta^H \Lambda_s^{-\frac{1}{2}} \mathbf{Q}_s^H [\mathbf{R}_{S_i} + \mathbf{R}_M] \mathbf{Q}_s \Lambda_s^{-\frac{1}{2}} \mathbf{Q}_\beta$$

where \mathbf{R}_{S_i} and \mathbf{R}_M denote respectively the covariance matrices of $\underline{S}_n^{(u)}$ and $\underline{M}_n^{(u)}$.

From (17) and (18), we have

$$\begin{aligned} \frac{1}{2} E \left\{ S_{n,q_1}^{(u)} S_{n,q_2}^{*(u)} \right\} &= 2\rho_u \sum_{l=1, l \neq q_1, l \neq q_2}^{L_u} \frac{1}{2} E \left\{ \alpha_l^{(u)} \alpha_l^{*(u)} \right\} \cdot \\ &\left[d_{m_1+1} d_{m_2+1} R_{u,u}(\tau'_{u,l;u,q_1}) R_{u,u}^*(\tau'_{u,l;u,q_2}) E \left\{ e^{j(\phi_{n-m_2-1}^{(u)} - \phi_{n-m_1-1}^{(u)})} \right\} \right. \\ &+ d_{m_1} d_{m_2+1} \hat{R}_{u,u}(\tau'_{u,l;u,q_1}) R_{u,u}^*(\tau'_{u,l;u,q_2}) E \left\{ e^{j(\phi_{n-m_2-1}^{(u)} - \phi_{n-m_1}^{(u)})} \right\} \\ &+ d_{m_1+1} d_{m_2} R_{u,u}(\tau'_{u,l;u,q_1}) \hat{R}_{u,u}^*(\tau'_{u,l;u,q_2}) E \left\{ e^{j(\phi_{n-m_2}^{(u)} - \phi_{n-m_1-1}^{(u)})} \right\} \\ &\left. + d_{m_1} d_{m_2} \hat{R}_{u,u}(\tau'_{u,l;u,q_1}) \hat{R}_{u,u}^*(\tau'_{u,l;u,q_2}) E \left\{ e^{j(\phi_{n-m_2}^{(u)} - \phi_{n-m_1}^{(u)})} \right\} \right] \end{aligned} \quad (52)$$

where $m_i = \lfloor (\tau_l^{(u)} - \tau_{q_i}^{(u)}) / T_b \rfloor$ for $i=1,2$. Similarly, we have

$$\begin{aligned} \frac{1}{2} E \left\{ M_{n,q_1}^{(u)} M_{n,q_2}^{*(u)} \right\} &= \sum_{k=1, k \neq u}^K 2\rho_k \sum_{l=1}^{L_k} \frac{1}{2} E \left\{ \alpha_l^{(k)} \alpha_l^{*(k)} \right\} \cdot \\ &\left[R_{k,u}(\tau'_{k,l;u,q_1}) R_{k,u}^*(\tau'_{k,l;u,q_2}) E \left\{ e^{j(\phi_{n-m_2-1}^{(k)} - \phi_{n-m_1-1}^{(k)})} \right\} \right. \\ &+ \hat{R}_{k,u}(\tau'_{k,l;u,q_1}) R_{k,u}^*(\tau'_{k,l;u,q_2}) E \left\{ e^{j(\phi_{n-m_2-1}^{(k)} - \phi_{n-m_1}^{(k)})} \right\} \\ &+ R_{k,u}(\tau'_{k,l;u,q_1}) \hat{R}_{k,u}^*(\tau'_{k,l;u,q_2}) E \left\{ e^{j(\phi_{n-m_2}^{(k)} - \phi_{n-m_1-1}^{(k)})} \right\} \\ &\left. + \hat{R}_{k,u}(\tau'_{k,l;u,q_1}) \hat{R}_{k,u}^*(\tau'_{k,l;u,q_2}) E \left\{ e^{j(\phi_{n-m_2}^{(k)} - \phi_{n-m_1}^{(k)})} \right\} \right] \end{aligned} \quad (53)$$

where $m_i = \lfloor (\tau_l^{(k)} - \tau_{q_i}^{(k)}) / T_b \rfloor$ for $i=1,2$.

The expectation involved in (52) and (53) can be evaluated as

$$E \left\{ e^{j(\phi_{n-r_2}^{(u)} - \phi_{n-r_1}^{(u)})} \right\} = \begin{cases} 1, & \text{if } r_2 = r_1 \\ 0, & \text{otherwise} \end{cases}$$

where r_1 and r_2 are taken from the sets of $\{m_1, m_1 + 1\}$ and $\{m_2, m_2 + 1\}$, respectively.

C Evaluation of $\mathbf{R}_F^{(up)}(i)$ and $\mathbf{R}_F^{(low)}(i)$

Generally, the covariance matrix of $F(i)$ can be expressed as

$$\mathbf{R}_F(i) = \mathbf{Q}_\beta^H \Lambda_s^{-\frac{1}{2}} \mathbf{Q}_s^H [\mathbf{R}_{\tilde{S}_i}(i-1) + \mathbf{R}_{\tilde{M}}(i-1)] \mathbf{Q}_s \Lambda_s^{-\frac{1}{2}} \mathbf{Q}_\beta$$

where $\mathbf{R}_{\tilde{S}_i}(i-1)$ and $\mathbf{R}_{\tilde{M}}(i-1)$ denote respectively the covariance matrices of $\tilde{S}_{i_n}^{(u)}(i-1)$ and $\tilde{M}_{i_n}^{(u)}(i-1)$.

Considering the channel estimation error for $\alpha_l^{(k)}$ in $\hat{S}_{i_n,q}^{(u)}(i-1)$ and $\hat{M}_{i_n,q}^{(k)}(i-1)$, we have

$$\begin{aligned} \tilde{S}_{i_n,q}^{(u)}(i-1) &= \sqrt{2\rho_u} \sum_{l=1, l \neq q}^{L_u} \alpha_l^{(u)} \left[d_{m+1} \left(e^{-j\hat{\phi}_{n-m-1}^{(u)}} - e^{-j\hat{\phi}_{n-m-1}^{(u)}(i-1)} \right) R_{u,u}(\tau'_{u,l;u,q}) \right. \\ &\quad \left. + d_m \left(e^{-j\hat{\phi}_{n-m}^{(u)}} - e^{-j\hat{\phi}_{n-m}^{(u)}(i-1)} \right) \hat{R}_{u,u}(\tau'_{u,l;u,q}) \right] \\ &\quad - \sqrt{2\rho_u} \sum_{l=1, l \neq q}^{L_u} \Delta \alpha_l^{(u)} \left[d_{m+1} e^{-j\hat{\phi}_{n-m-1}^{(u)}(i-1)} R_{u,u}(\tau'_{u,l;u,q}) \right. \\ &\quad \left. + d_m e^{-j\hat{\phi}_{n-m}^{(u)}(i-1)} \hat{R}_{u,u}(\tau'_{u,l;u,q}) \right] \end{aligned}$$

and

$$\begin{aligned} \tilde{M}_{i_n,q}^{(u)}(i-1) &= \sum_{k=1, k \neq u}^K \sqrt{2\rho_k} \sum_{l=1}^{L_k} \alpha_l^{(k)} \left[\left(e^{-j\hat{\phi}_{n-m-1}^{(k)}} - e^{-j\hat{\phi}_{n-m-1}^{(k)}(i-1)} \right) R_{k,u}(\tau'_{k,l;u,q}) \right. \\ &\quad \left. + \left(e^{-j\hat{\phi}_{n-m}^{(k)}} - e^{-j\hat{\phi}_{n-m}^{(k)}(i-1)} \right) \hat{R}_{k,u}(\tau'_{k,l;u,q}) \right] \\ &\quad - \sum_{k=1, k \neq u}^K \sqrt{2\rho_k} \sum_{l=1}^{L_k} \Delta \alpha_l^{(k)} \left[e^{-j\hat{\phi}_{n-m-1}^{(k)}(i-1)} R_{k,u}(\tau'_{k,l;u,q}) \right. \\ &\quad \left. + e^{-j\hat{\phi}_{n-m}^{(k)}(i-1)} \hat{R}_{k,u}(\tau'_{k,l;u,q}) \right] \end{aligned}$$

As a result, we obtain

$$\begin{aligned}
\frac{1}{2}E \left\{ \tilde{S}_{i_{n,q_1}}^{(u)}(i-1) \tilde{S}_{i_{n,q_2}}^{*(u)}(i-1) \right\} &= 2\rho_u \sum_{l=1, l \neq q_1, l \neq q_2}^{L_u} \frac{1}{2}E \{ [\Delta \alpha_l^{(u)}][\Delta \alpha_l^{*(u)}] \} \cdot \\
&\left[d_{m_1+1} d_{m_2+1} R_{u,u}(\tau'_{u,l;u,q_1}) R_{u,u}^*(\tau'_{u,l;u,q_2}) \hat{E}_{m_1+1, m_2+1}^{(u)} \right. \\
&+ d_{m_1} d_{m_2+1} \hat{R}_{u,u}(\tau'_{u,l;u,q_1}) R_{u,u}^*(\tau'_{u,l;u,q_2}) \hat{E}_{m_1, m_2+1}^{(u)} \\
&+ d_{m_1+1} d_{m_2} R_{u,u}(\tau'_{u,l;u,q_1}) \hat{R}_{u,u}^*(\tau'_{u,l;u,q_2}) \hat{E}_{m_1+1, m_2}^{(u)} \\
&\left. + d_{m_1} d_{m_2} \hat{R}_{u,u}(\tau'_{u,l;u,q_1}) \hat{R}_{u,u}^*(\tau'_{u,l;u,q_2}) \hat{E}_{m_1, m_2}^{(u)} \right] \\
&+ 2\rho_u \sum_{l=1, l \neq q_1, l \neq q_2}^{L_u} \frac{1}{2}E \{ \alpha_l^{(u)} \alpha_l^{*(u)} \} \cdot \\
&\left[d_{m_1+1} d_{m_2+1} R_{u,u}(\tau'_{u,l;u,q_1}) R_{u,u}^*(\tau'_{u,l;u,q_2}) E_{m_1+1, m_2+1}^{(u)} \right. \\
&+ d_{m_1} d_{m_2+1} \hat{R}_{u,u}(\tau'_{u,l;u,q_1}) R_{u,u}^*(\tau'_{u,l;u,q_2}) E_{m_1, m_2+1}^{(u)} \\
&+ d_{m_1+1} d_{m_2} R_{u,u}(\tau'_{u,l;u,q_1}) \hat{R}_{u,u}^*(\tau'_{u,l;u,q_2}) E_{m_1+1, m_2}^{(u)} \\
&\left. + d_{m_1} d_{m_2} \hat{R}_{u,u}(\tau'_{u,l;u,q_1}) \hat{R}_{u,u}^*(\tau'_{u,l;u,q_2}) E_{m_1, m_2}^{(u)} \right]
\end{aligned}$$

where $m_i = \lfloor (\tau_l^{(u)} - \tau_{q_i}^{(u)})/T_b \rfloor$ for $i=1,2$. Also, we have

$$\begin{aligned}
\frac{1}{2}E \left\{ \tilde{M}_{n,q_1}^{(u)}(i-1) \tilde{M}_{n,q_2}^{*(u)}(i-1) \right\} &= \sum_{k=1, k \neq u}^K 2\rho_k \sum_{l=1}^{L_k} \frac{1}{2}E \{ [\Delta \alpha_l^{(k)}][\Delta \alpha_l^{*(k)}] \} \cdot \\
&\left[R_{k,u}(\tau'_{k,l;u,q_1}) R_{k,u}^*(\tau'_{k,l;u,q_2}) \hat{E}_{m_1+1, m_2+1}^{(k)} \right. \\
&+ \hat{R}_{k,u}(\tau'_{k,l;u,q_1}) R_{k,u}^*(\tau'_{k,l;u,q_2}) \hat{E}_{m_1, m_2+1}^{(k)} \\
&+ R_{k,u}(\tau'_{k,l;u,q_1}) \hat{R}_{k,u}^*(\tau'_{k,l;u,q_2}) \hat{E}_{m_1+1, m_2}^{(k)} \\
&\left. + \hat{R}_{k,u}(\tau'_{k,l;u,q_1}) \hat{R}_{k,u}^*(\tau'_{k,l;u,q_2}) \hat{E}_{m_1, m_2}^{(k)} \right] \\
&+ \sum_{k=1, k \neq u}^K 2\rho_k \sum_{l=1}^{L_k} \frac{1}{2}E \{ \alpha_l^{(k)} \alpha_l^{*(k)} \} \cdot \\
&\left[R_{k,u}(\tau'_{k,l;u,q_1}) R_{k,u}^*(\tau'_{k,l;u,q_2}) E_{m_1+1, m_2+1}^{(k)} \right. \\
&+ \hat{R}_{k,u}(\tau'_{k,l;u,q_1}) R_{k,u}^*(\tau'_{k,l;u,q_2}) E_{m_1, m_2+1}^{(k)} \\
&+ R_{k,u}(\tau'_{k,l;u,q_1}) \hat{R}_{k,u}^*(\tau'_{k,l;u,q_2}) E_{m_1+1, m_2}^{(k)} \\
&\left. + \hat{R}_{k,u}(\tau'_{k,l;u,q_1}) \hat{R}_{k,u}^*(\tau'_{k,l;u,q_2}) E_{m_1, m_2}^{(k)} \right]
\end{aligned}$$

where $m_i = \lfloor (\tau_l^{(k)} - \tau_{q_i}^{(k)})/T_b \rfloor$ for $i=1,2$.

The expectations $\hat{E}_{r_1, r_2}^{(k)}$ and $E_{r_1, r_2}^{(k)}$ are

$$\hat{E}_{r_1, r_2}^{(k)} = E \{ e^{j[\hat{\phi}_{n-r_2}^{(k)}(i-1) - \hat{\phi}_{n-r_1}^{(k)}(i-1)]} \} = \begin{cases} 1, & \text{if } r_2 = r_1 \\ 0, & \text{otherwise} \end{cases}$$

and

$$\begin{aligned}
E_{r_1, r_2}^{(k)} &= E \left\{ \left[e^{-j\phi_{n-r_1}^{(k)}} - e^{-j\hat{\phi}_{n-r_1}^{(k)}(i-1)} \right] \left[e^{-j\phi_{n-r_2}^{(k)}} - e^{-j\hat{\phi}_{n-r_2}^{(k)}(i-1)} \right]^* \right\} \\
&= \begin{cases} \frac{1}{4} \sum_{p=1}^4 \sum_{\hat{p}=1, \hat{p} \neq p}^4 g_1(p, \hat{p}) & \text{if } r_1 = r_2 = r \\ \frac{1}{16} \sum_{p_1=1}^4 \sum_{\hat{p}_1=1, \hat{p}_1 \neq p_1}^4 \sum_{p_2=1}^4 \sum_{\hat{p}_2=1, \hat{p}_2 \neq p_2}^4 g_2(p_1, p_2, \hat{p}_1, \hat{p}_2) & \text{otherwise} \end{cases}
\end{aligned}$$

Here, r_1 and r_2 are taken from the sets of $\{m_1, m_1 + 1\}$ and $\{m_2, m_2 + 1\}$, respectively, and

$$\begin{aligned}
g_1(p, \hat{p}) &= \left[e^{-j\psi_p} - e^{-j\psi_{\hat{p}}} \right] \left[e^{-j\psi_p} - e^{-j\psi_{\hat{p}}} \right]^* P_s \left\{ \hat{\phi}_{n-r}^{(k)}(i-1) = \psi_{\hat{p}} | \phi_{n-r}^{(k)} = \psi_p \right\} \\
g_2(p_1, p_2, \hat{p}_1, \hat{p}_2) &= \left[e^{-j\psi_{p_1}} - e^{-j\psi_{\hat{p}_1}} \right] \left[e^{-j\psi_{p_2}} - e^{-j\psi_{\hat{p}_2}} \right]^* P_s \left\{ \hat{\phi}_{n-r_1}^{(k)}(i-1) = \psi_{\hat{p}_1} | \phi_{n-r_1}^{(k)} = \psi_{p_1} \right\} \cdot \\
&\quad P_s \left\{ \hat{\phi}_{n-r_2}^{(k)}(i-1) = \psi_{\hat{p}_2} | \phi_{n-r_2}^{(k)} = \psi_{p_2} \right\}
\end{aligned}$$

$\psi_p := 2\pi(p-1)/4$ is the possible phase shift, and $P_s \{ \hat{\phi}_n^{(k)}(i-1) = \psi_{\hat{p}} | \phi_n^{(k)} = \psi_p \}$ is the symbol error probability when $\phi_n^{(k)} = \psi_p$ is transmitted while the tentative decision in the $(i-1)$ -th stage is $\psi_{\hat{p}}$.

For user k , let $X^{(k)}(i-1)$ be the combiner output in the $(i-1)$ -th stage. Thus, $P_s \{ \hat{\phi}_n^{(k)}(i-1) = \psi_{\hat{p}} | \phi_n^{(k)} = \psi_p \} = \Pr \{ X^{(k)}(i-1) e^{j\psi_p} \in R_t \} = A_t$, where R_t is the region containing the vector $e^{j(\hat{\phi}_n^{(k)}(i-1) - \phi_n^{(k)})}$ [31].

Following the approach in [31], we have

$$\begin{aligned}
A_1 &= \mathcal{F}(\gamma = -\pi/4) \mathcal{F}(\gamma = -3\pi/4) \\
A_2 &= \mathcal{F}(\gamma = -\pi/4) \mathcal{F}(\gamma = \pi/4) \\
A_3 &= \mathcal{F}(\gamma = \pi/4) \mathcal{F}(\gamma = 3\pi/4)
\end{aligned} \tag{54}$$

where $\mathcal{F}(\gamma) := \Pr \{ X^{(k)}(i-1) e^{j\psi_p} e^{j\gamma} < 0 \}$.

When the bit error rate is irrelevant or weakly dependent on $\psi_{\hat{p}}$, we may evaluate (54) by setting $\psi_p=0$ and we have

$$\begin{aligned}
\mathcal{F}(\gamma = \pi/4) &= \mathcal{F}(\gamma = -\pi/4) \\
\mathcal{F}(\gamma = -3\pi/4) &= \mathcal{F}(\gamma = 3\pi/4) = 1 - \mathcal{F}(\gamma = -\pi/4)
\end{aligned} \tag{55}$$

where $\mathcal{F}(\gamma = -\pi/4)$ is the bit error rate of user k in the $(i-1)$ -th stage. One can readily check that by substituting (54) and (55) into (32), $R_b = \mathcal{F}(\gamma = -\pi/4)$ follows.

As previously mentioned, due to the correlated residual interference, the exact evaluation of $\mathcal{F}(\gamma = -\pi/4)$ is quite difficult and thus the upper and lower bounds in $(i-1)$ -th stage denoted by $P_b^{(up)}(i-1)$ and $P_b^{(low)}(i-1)$, respectively, are derived in Section 4.2. In addition, by using the Gaussian approximation for the interference, these upper and lower bounds on the BER are irrelevant to the transmitted symbols. Therefore, instead of computing the exact $\mathbf{R}_F(i)$, we may compute $\mathbf{R}_F^{(up)}(i)$ and $\mathbf{R}_F^{(low)}(i)$ relying on $P_b^{(up)}(i-1)$ and $P_b^{(low)}(i-1)$, respectively. In particular, by letting $\mathcal{F}(\gamma = -\pi/4) = P_b^{(up)}(i-1)$ in (55) for all users, the resulting $\mathbf{R}_F(i)$ is referred to as $\mathbf{R}_F^{(up)}(i)$, while letting $\mathcal{F}(\gamma = -\pi/4) = P_b^{(low)}(i-1)$ for all users, we obtain $\mathbf{R}_F^{(low)}(i)$.

References

- [1] Y. C. Yoon, R. Kohno, and H. Imai, "A spread-spectrum multiaccess system with cochannel interference cancellation for multipath fading channels," *IEEE J. Select. Areas Commun.*, vol. SAC-11, pp. 1067–1075, Sept. 1993.
- [2] A. L. C. Hui and K. B. Letaief, "Successive interference cancellation for multiuser asynchronous DS/CDMA detectors in multipath fading links," *IEEE Trans. Commun.*, vol. COM-46, pp. 384–391, Mar. 1998.
- [3] J. G. Proakis, *Digital communications*. New York: McGraw-Hill, 1995.
- [4] R. L. Pickholtz, L. B. Milstein, and D. L. Schilling, "Spread spectrum for mobile communications," *IEEE Trans. Vehi. Tech.*, vol. VT-40, pp. 313–321, May 1991.
- [5] S. Verdu, "Minimum probability of error for asynchronous Gaussian multiple access channels," *IEEE Trans. Inform. Theo.*, vol. IT-32, pp. 85–96, Jan. 1986.
- [6] R. Lupas and S. Verdu, "Near-far resistance of multiuser detectors in asynchronous channels," *IEEE Trans. Commun.*, vol. COM-38, pp. 496–508, Sep. 1990.
- [7] M. K. Varanasi and B. Aazhang, "Multistage detection in asynchronous code-division multiple-access communications," *IEEE Trans. Commun.*, vol. COM-38, pp. 509–519, April 1990.
- [8] T. Miyajima, T. Hasegawa, and M. Haneishi, "On the multiuser detection using a neural network in code-division multiple-access communications," *IEICE Trans. Commun.*, vol. E76-B, pp. 961–968, Aug. 1993.
- [9] M. K. Varanasi, "Noncoherent detection in asynchronous multiuser channels," *IEEE Trans. Inform. Theo.*, vol. IT-39, pp. 157–176, Jan. 1993.
- [10] P. Patel and J. Holtzman, "Analysis of a simple successive interference cancellation scheme in a DS/CDMA system," *IEEE J. Select. Areas Commun.*, vol. SAC-12, pp. 796–807, June 1994.
- [11] A. Kajiwarra and M. Nakagawa, "Microcellular CDMA system with a linear multiuser interference canceler," *IEEE J. Select. Areas Commun.*, vol. SAC-12, pp. 605–611, May 1994.
- [12] L. B. Nelson and H. V. Poor, "Iterative multiuser receivers for CDMA channels: an EM-based approach," *IEEE Trans. Commun.*, vol. COM-44, pp. 1700–1710, Dec 1996.
- [13] U. Madhow and M. L. Honig, "MMSE interference suppression for direct sequence spread spectrum CDMA," *IEEE Trans. Commun.*, vol. COM-42, pp. 3178–3188, Dec. 1994.

- [14] U. Mitra and H. V. Poor, "Adaptive receiver algorithms for near-far resistant CDMA," *IEEE Trans. Commun.*, vol. COM-43, pp. 1713–1724, Feb./Mar./April 1995.
- [15] S. Verdu, "Adaptive multiuser detection," *Proc. IEEE 3rd Int. Symp. Spread Spectrum Tech. and Appl., ISSSTA'94*, (Oulu, Finland), pp. 43–50, July 1994.
- [16] D. Chen and S. Roy, "An adaptive multiuser receiver for CDMA systems," *IEEE J. Select. Areas Commun.*, vol. SAC-12, pp. 808–816, June 1994.
- [17] U. Fawer and B. Aazhang, "A multiuser receiver for code division multiple access communication over multipath channels," *IEEE Trans. Commun.*, vol. COM-43, pp. 1556–1565, Feb./Mar./April 1995.
- [18] Z. Zvonar, "Combined multiuser detection and diversity reception for wireless CDMA systems," *IEEE Trans. Vehi. Tech.*, vol. VT-45, pp. 205–211, Feb. 1996.
- [19] D. Divsalar and M. Simon, "Improved CDMA performance using parallel interference cancellation," tech. rep., JPL, California Institute of Technology, CA, USA, Oct. 1995.
- [20] S. Moshavi, "Multiuser detector for DS-CDMA communications," *IEEE Commun. Magazine*, pp. 124–136, Oct. 1996.
- [21] A. E. Brand and A. H. Aghvami, "Performance of a joint CDMA/PRMA proposal for mixed voice/data transmission for third generation mobile communications," *IEEE J. Select. Areas Commun.*, vol. SAC-14, pp. 1698–1707, Dec. 1996.
- [22] W. B. Yang and E. Geraniotis, "Admission policies for integrated voice and data traffic in CDMA packet radio networks," *IEEE J. Select. Areas Commun.*, vol. SAC-12, pp. 654–664, May 1994.
- [23] S. Striglis, A. Kaul, N. Yang, and B. D. Woerner, "A multistage RAKE receiver for improved capacity of CDMA systems," *Proc. IEEE Vehi. Tech. Conf., VTC94, Stockholm, Sweden*, pp. 789–793, June 1994.
- [24] R. L. Peterson, R. E. Ziemer, and D. E. Borth, *Introduction to spread spectrum communications*. London: Prentice-Hall, Inc., 1995.
- [25] G. D. Boudreau, D. D. Falconer, and S. A. Mahmoud, "A comparison of trellis coded versus convolutionally coded spread spectrum multiple-access system," *IEEE J. Select. Areas Commun.*, vol. SAC-8, pp. 628–640, May 1990.
- [26] R. A. Iltis and L. Mailaender, "An adaptive multiuser detector with joint amplitude and delay estimation," *IEEE J. Select. Areas Commun.*, vol. SAC-12, pp. 774–785, June 1994.

- [27] R. A. Iltis, "A GLRT-based spread spectrum receiver for joint channel estimation and interference suppression," *IEEE Trans. Commun.*, vol. COM-37, pp. 277–288, Mar. 1989.
- [28] M. B. Pursley, "Performance evaluation for phase-coded spread-spectrum multiple access communication - part I: system analysis," *IEEE Trans. Commun.*, vol. COM-25, pp. 795–799, Aug. 1977.
- [29] J. Panicker and S. Kumar, "Effect of system imperfections on BER performance of a CDMA receiver with multipath diversity combining," *IEEE Trans. Vehi. Tech.*, vol. VT-45, pp. 622–630, Nov 1996.
- [30] A. Papoulis, *Probability, random variables, and stochastic processes*. New York: McGraw-Hill, 1991.
- [31] P. Y. Kam, "Bit error probability of MDPSK over the non-selective Rayleigh fading channels with diversity reception," *IEEE Trans. Commun.*, vol. COM-39, pp. 220–224, Feb. 1991.
- [32] M. Schwartz, W. R. Bennett, and S. Stein, *Communication systems and techniques*. New York: McGraw-Hill, 1966.
- [33] J. F. Weng, *Performance of two-stage nonlinear detector in DS/CDMA system with impulse noise*. PhD thesis, Dept. of Electronic Eng., City Univ. of Hong Kong, Hong Kong, Aug. 1997.
- [34] M. B. Pursley and H. F. A. Roefs, "Numerical evaluation of correlation parameters for optimal phases of binary shift-register sequences," *IEEE Trans. Commun.*, vol. COM-27, pp. 1597–1604, Oct. 1979.

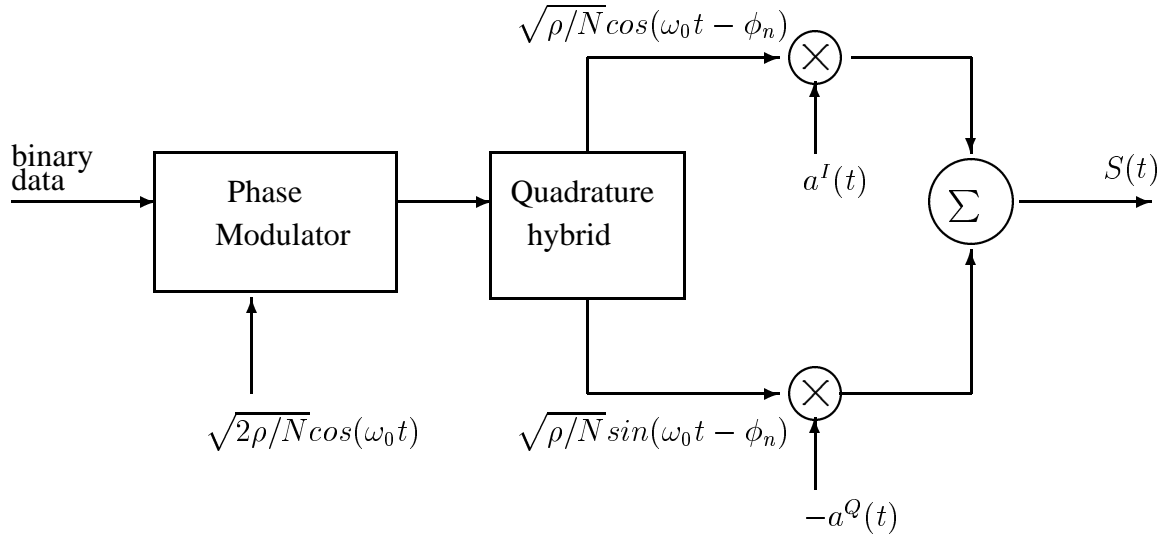


Fig. 1: Balanced QPSK transmitter model

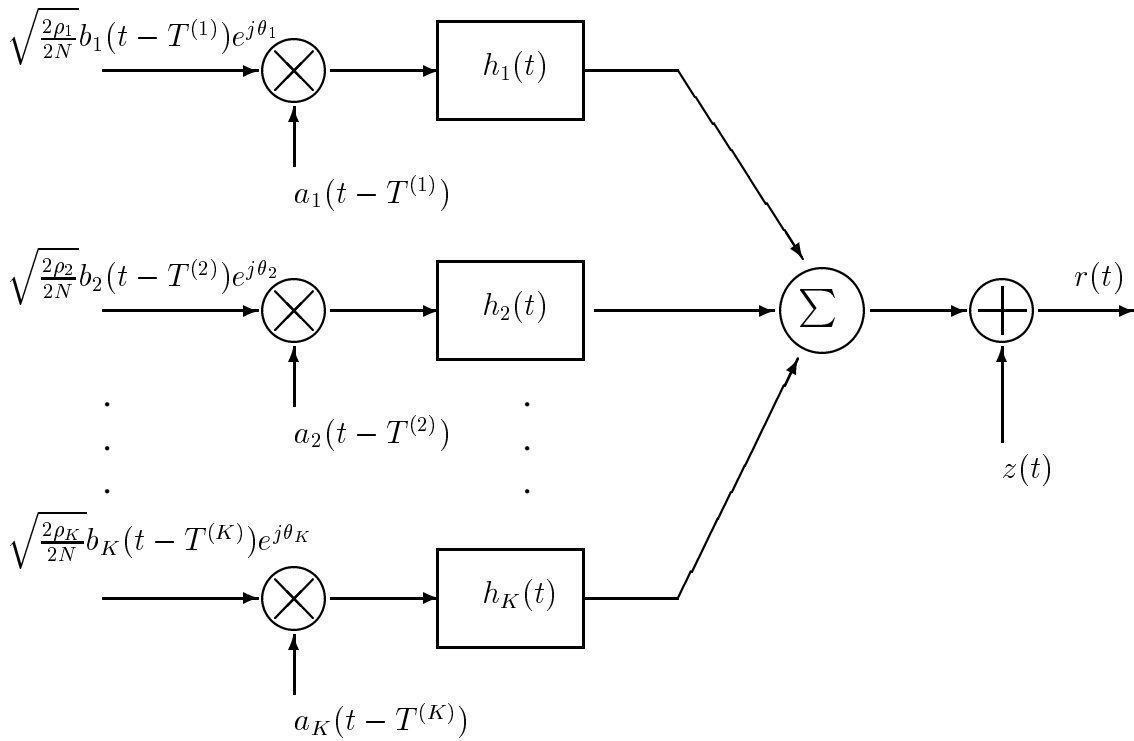


Fig. 2: Equivalent low-pass transmitter and channel model

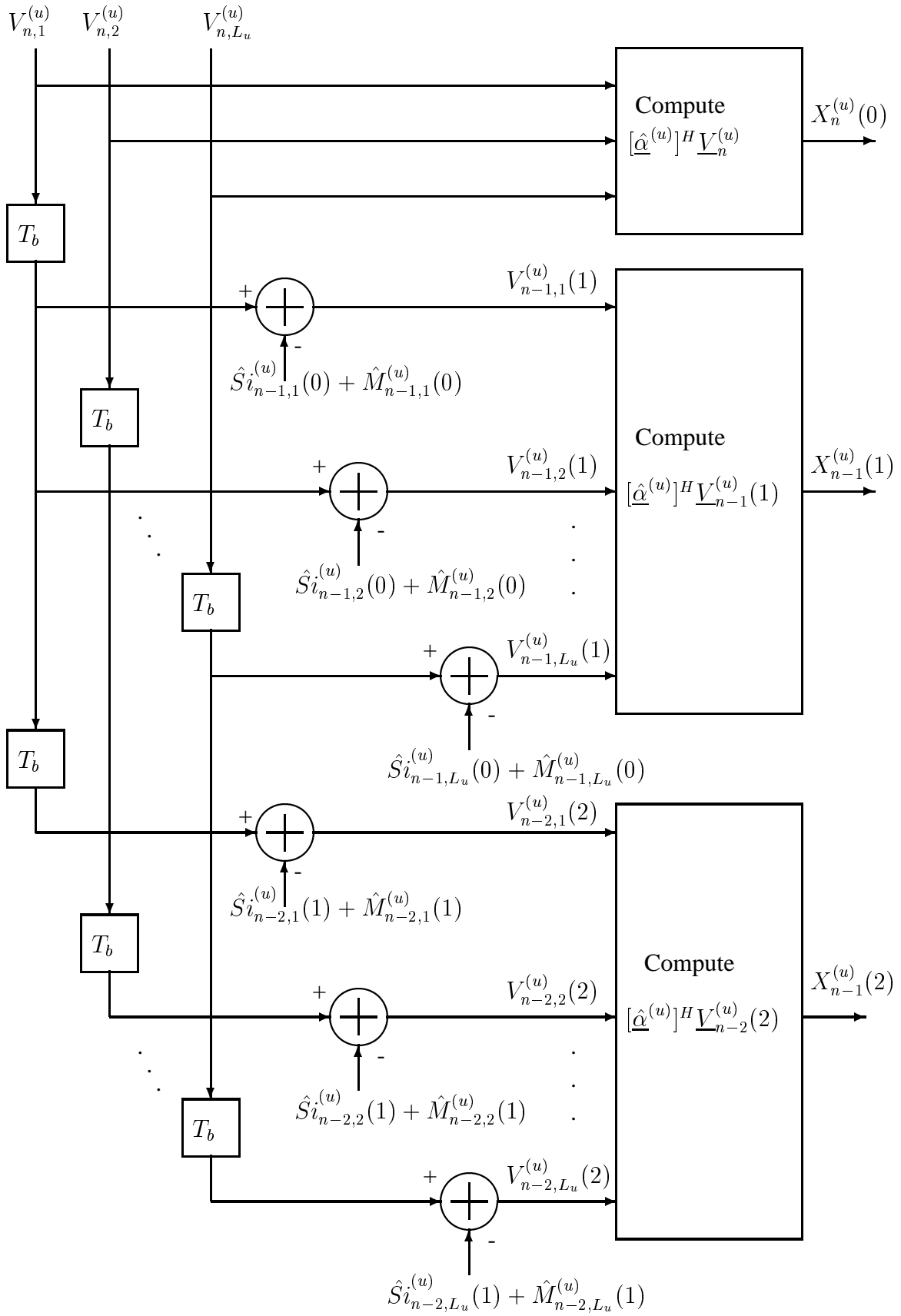


Fig. 3: Structure of the proposed 2-stage MIC-PSI for user u

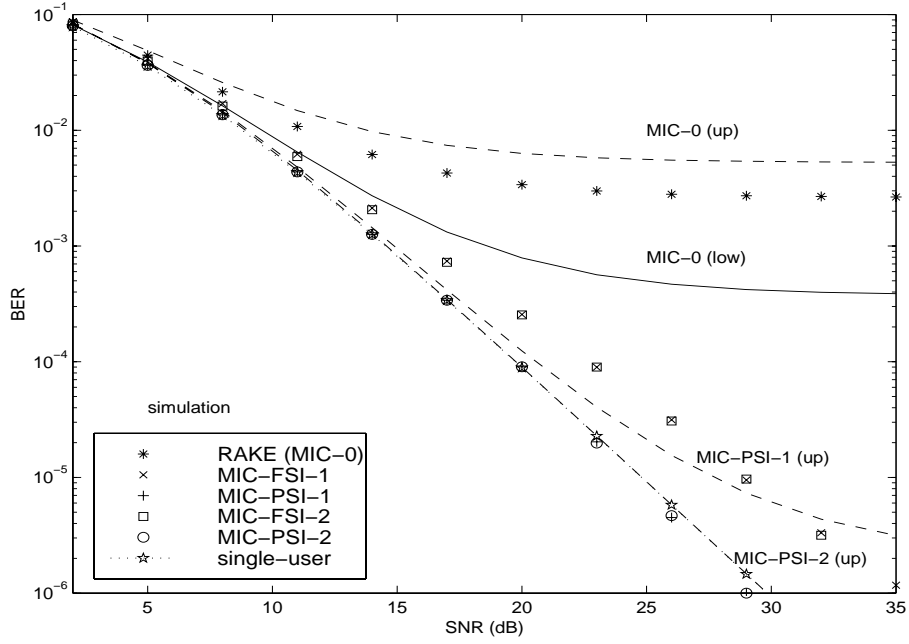


Fig. 4: Analytical and simulation results on the BER of the MIC schemes versus SNR in a 3-user system over a 2-path Rayleigh fading channel. ($N=31$, equal-power users). Dashed lines: analytical upper bound. Solid lines: analytical lower bound.

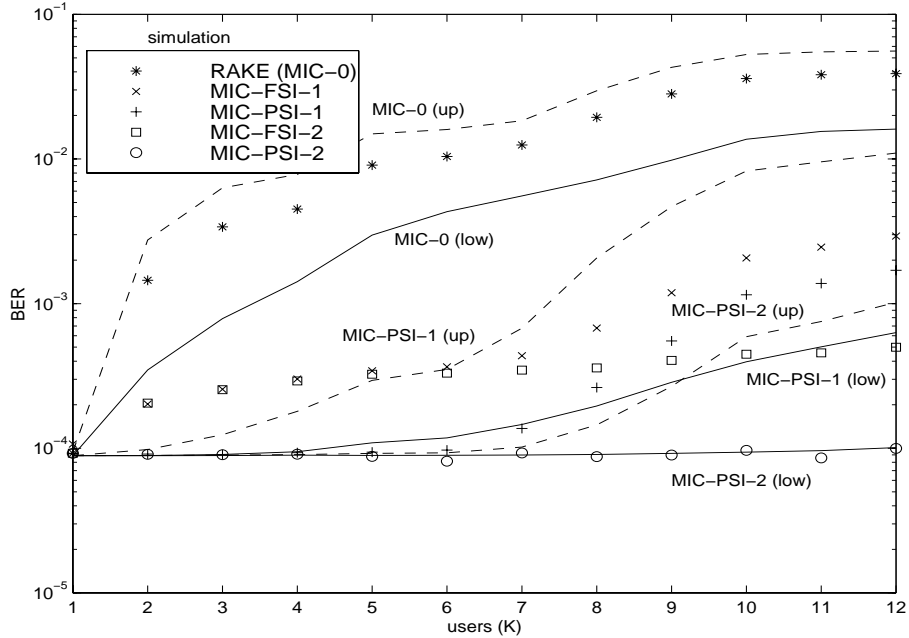


Fig. 5: Analytical and simulation results on the BER of the MIC schemes versus the number of users (K) at SNR=20dB and $N=31$ over a 2-path Rayleigh fading channel. Equal-power users. Dashed lines: analytical upper bound. Solid lines: analytical lower bound.

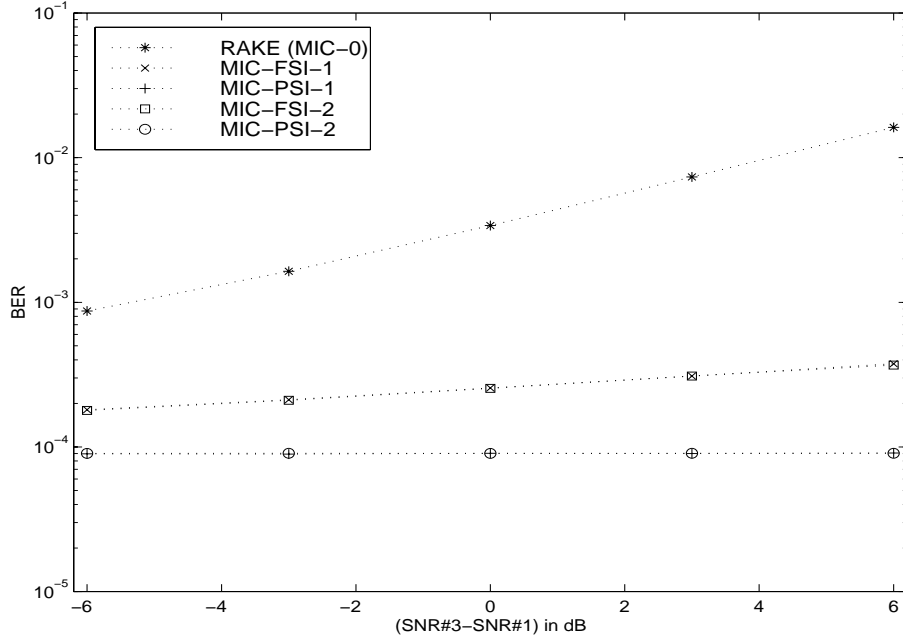


Fig. 6: Simulation results on the BER of the MIC schemes versus $(\text{SNR}\#3-\text{SNR}\#1)$ in a 3-user system over a 2-path Rayleigh fading channel. $\text{SNR}\#1=20\text{dB}$, $\text{SNR}\#2=(\text{SNR}\#3+\text{SNR}\#1)/2$, $N=31$.

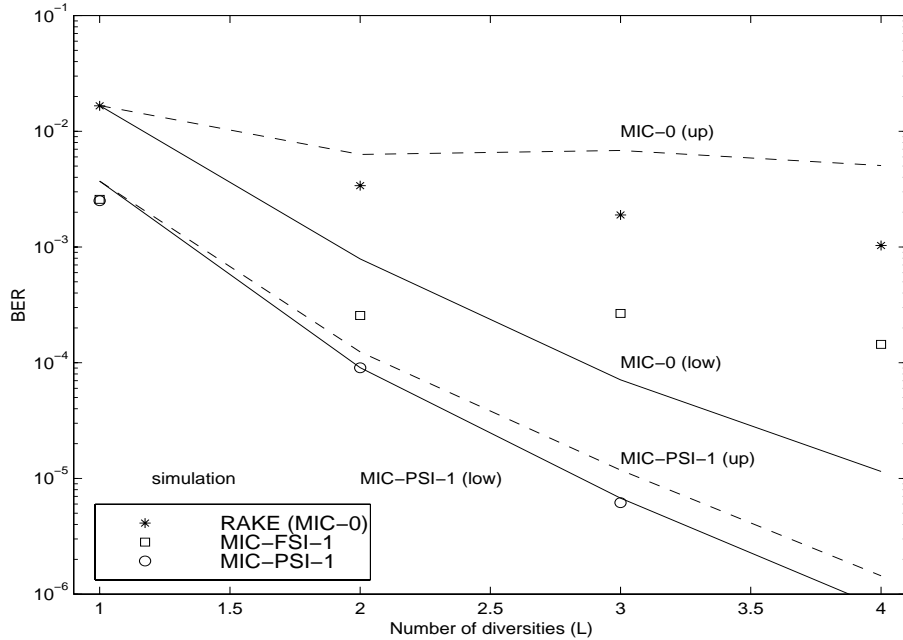


Fig. 7: Analytical and simulation results on the BER of the MIC schemes versus the number of diversities (L) in a 3-user system over multipath Rayleigh fading channels. $\text{SNR}=20\text{dB}$, $N=31$, equal-power users. Dashed lines: analytical upper bound. Solid lines: analytical lower bound.

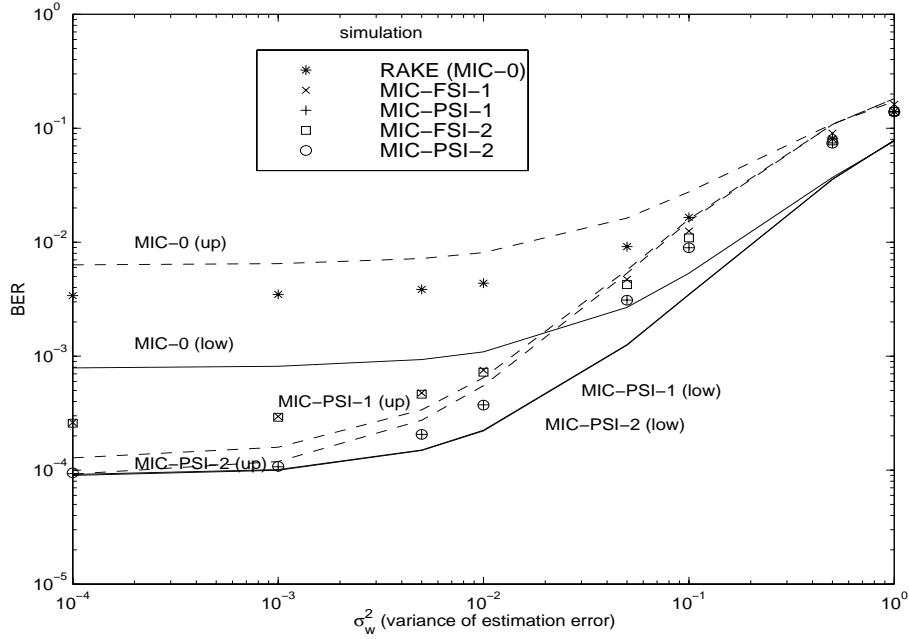


Fig. 8: Analytical and simulation results on the BER of the MIC schemes versus the variance of the estimation error in a 3-user system over a 2-path Rayleigh fading channel. SNR=20dB, $N=31$, equal-power users. Dashed lines: analytical upper bound. Solid lines: analytical lower bound.

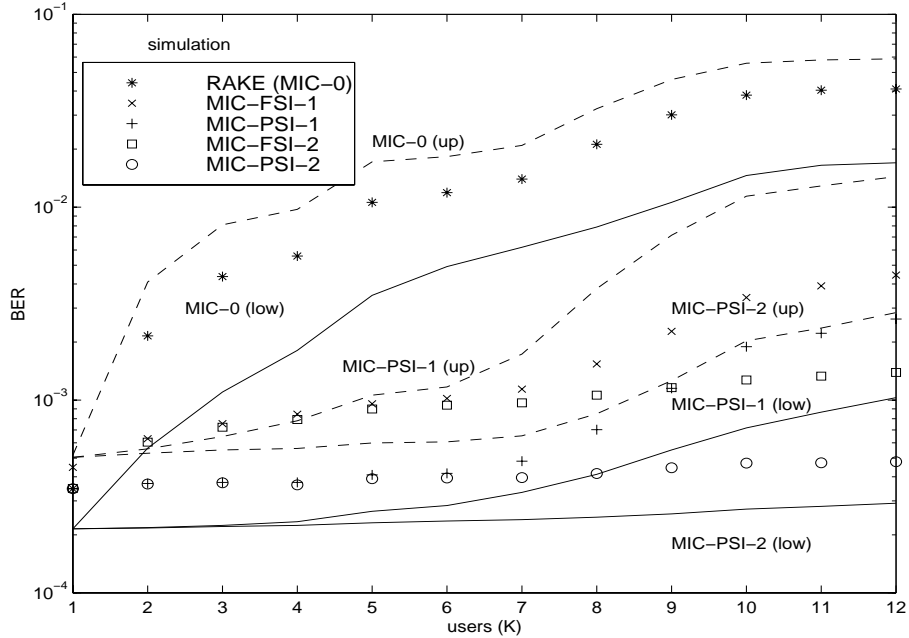


Fig. 9: Analytical and simulation results on the BER of the MIC schemes versus the number of users (K) in a multi-user system over a 2-path Rayleigh fading channel. SNR=20dB, $N=31$, $\sigma_w^2 = 10^{-2}$, equal-power users. Dashed lines: analytical upper bound. Solid lines: analytical lower bound.

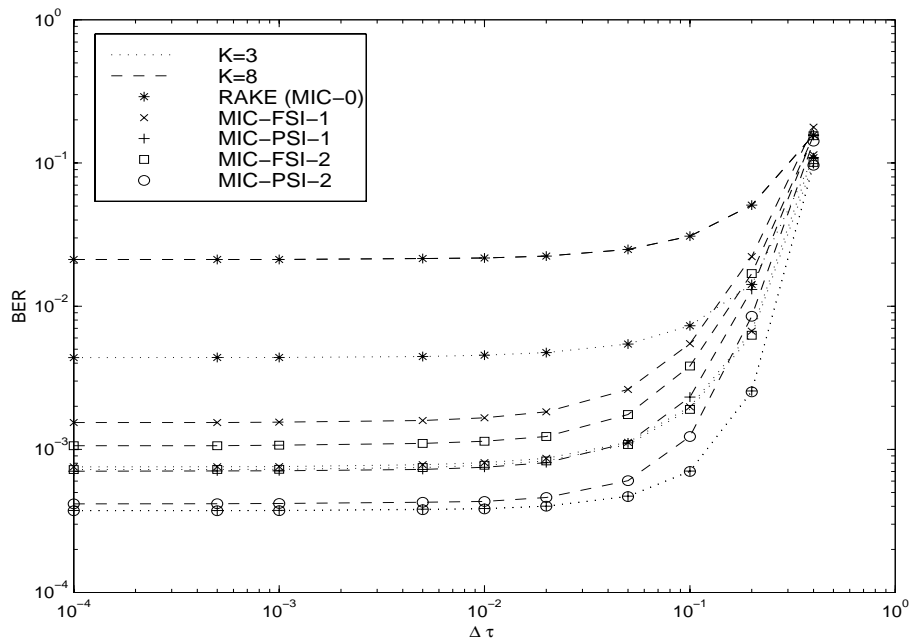


Fig. 10: Simulation results on the BER of the MIC schemes versus the time delay estimation error ($\Delta\tau$) in 3 and 8-user systems over a 2-path Rayleigh fading channel. SNR=20dB, $N=31$, $\sigma_w^2 = 10^{-2}$, equal-power users.